


Accepted Article Preview: Published ahead of advance online publication

	<p>The action of obestatin in skeletal muscle repair: stem cell expansion, muscle growth, and microenvironment remodeling</p>
	<p>Uxía Gurriarán-Rodríguez, Icíá Santos-Zas Jessica González-Sánchez, Daniel Beiroa, Viviana Moresi, Carlos S. Mosteiro, Wei Lin, Juan E Viñuela, José Señarís, Tomás García-Caballero, Felipe F. Casanueva, Rubén Nogueiras, Rosalía Gallego, Jean-Marc Renaud, Sergio Adamo, Yolanda Pazos and Jesús P. Camiña</p>
<p>Cite this article as: Uxía Gurriarán-Rodríguez, Icíá Santos-Zas Jessica González-Sánchez, Daniel Beiroa, Viviana Moresi, Carlos S. Mosteiro, Wei Lin, Juan E Viñuela, José Señarís, Tomás García-Caballero, Felipe F. Casanueva, Rubén Nogueiras, Rosalía Gallego, Jean-Marc Renaud, Sergio Adamo, Yolanda Pazos and Jesús P. Camiña, The action of obestatin in skeletal muscle repair: stem cell expansion, muscle growth, and microenvironment remodeling, <i>Molecular Therapy</i> accepted article preview online 12 March 2015; doi:10.1038/mt.2015.40</p>	
<p>This is a PDF file of an unedited peer-reviewed manuscript that has been accepted for publication. NPG is providing this early version of the manuscript as a service to our customers. The manuscript will undergo copyediting, typesetting and a proof review before it is published in its final form. Please note that during the production process errors may be discovered which could affect the content, and all legal disclaimers apply.</p>	
<p>Received 20 January 2014 accepted 29 January 2015; Accepted article preview online 12 March 2015</p>	

The action of obestatin in skeletal muscle repair: stem cell expansion, muscle growth, and microenvironment remodeling

Uxía Gurriarán-Rodríguez^{1,2,§}, Icíá Santos-Zas^{1,2}, Jessica González-Sánchez^{1,2}, Daniel Beiroa^{2,3}, Viviana Moresi^{4,5}, Carlos S. Mosteiro^{1,2}, Wei Lin⁶, Juan E Viñuela⁷, José Señarís⁸, Tomás García-Caballero⁹, Felipe F. Casanueva^{1,2,10}, Rubén Nogueiras^{2,3}, Rosalía Gallego⁹, Jean-Marc Renaud⁶, Sergio Adamo^{4,5}, Yolanda Pazos^{1,2} and Jesús P. Camiña^{1,2,*}

(1) Área de Endocrinología Molecular y Celular, Instituto de Investigación Sanitaria de Santiago (IDIS), Complejo Hospitalario Universitario de Santiago (CHUS), Servicio Gallego de Salud (SERGAS), Santiago de Compostela, Spain.

(2) CIBER Fisiopatología de la Obesidad y Nutrición, Spain.

(3) Departamento de Fisiología, Universidad de Santiago de Compostela (USC), Santiago de Compostela, Spain.

(4) Department of Anatomical, Histological, Forensic & Orthopaedic Sciences, Sapienza University of Rome, Rome, Italy.

(5) Interuniversity Institute of Myology, Rome, Italy.

(6) Department of Cellular and Molecular Medicine, University of Ottawa, Ottawa, Canada.

(7) Unidad de Inmunología, CHUS, Santiago de Compostela, Spain.

(8) Servicio de Cirugía Ortopédica y Traumatología, CHUS, SERGAS, Santiago de Compostela, Spain.

(9) Departamento de Ciencias Morfológicas, USC, Santiago de Compostela, Spain.

(10) Departamento de Medicina, USC, Santiago de Compostela, Spain.

Keywords: skeletal muscle | skeletal muscle regeneration | obestatin signaling

Short title: Obestatin improves skeletal muscle repair

*To whom correspondence should be addressed: Jesus P. Camiña, PhD. Laboratorio de Endocrinología Celular. IDIS. Hospital Clínico Universitario de Santiago. Trav. Coupana s/n. 15706 Santiago de Compostela. Spain. Tel.: 0034981955072; E-mail: jesus.perez@usc.es

§Present address: Sprott Centre for Stem Cell Research, Ottawa Health Research Institute, Ottawa, Canada.

ABSTRACT

The development of therapeutic strategies for skeletal muscle diseases, such as physical injuries and myopathies, depends on the knowledge of regulatory signals that control the myogenic process. The obestatin/GPR39 system operates as an autocrine signal in the regulation of skeletal myogenesis. Using a mouse model of skeletal muscle regeneration after injury and several cellular strategies, we explored the potential use of obestatin as a therapeutic agent for the treatment of trauma-induced muscle injuries. Our results evidenced that the overexpression of the preproghrelin, and thus obestatin, and GPR39 in skeletal muscle increased regeneration after muscle injury. More importantly, the intramuscular injection of obestatin significantly enhanced muscle regeneration by stimulating satellite stem cell expansion as well as myofiber hypertrophy through a kinase hierarchy. Added to the myogenic action, the obestatin administration resulted in an increased expression of VEGF/VEGFR2 and the consequent microvascularization, with no effect on collagen deposition in skeletal muscle. Furthermore, the potential inhibition of myostatin during obestatin treatment might contribute to its myogenic action improving muscle growth and regeneration. Taken together, our data demonstrate successful improvement of muscle regeneration, indicating obestatin is a potential therapeutic agent for skeletal muscle injury and would benefit other myopathies related to muscle regeneration.

INTRODUCTION

Responding to injury, skeletal muscle undergoes an orchestrated process in which the activation of various cellular and molecular responses result in the reorganization of innervated, vascularized contractile muscle. This regenerative activity takes place in three sequential overlapping phases: 1) the inflammatory response; 2) the activation, differentiation, and fusion of satellite stem cells, the myogenic progenitors localized between the basal lamina and the muscle fiber membrane; and 3) the maturation and remodeling of newly formed myofibers (1). The necrosis of damaged muscle fibers is the initial step corresponding to the first stage of muscle degeneration. This event is initiated by dissolution of the myofiber sarcolemma, which leads to increased myofiber permeability. Myofiber necrosis also activates the complement cascade and induces inflammatory responses. Following to the inflammatory responses, chemotactic recruitment of circulating leukocytes occurs at the local sites of damage (2). The first inflammatory cells to infiltrate the damaged muscle are the neutrophils, which are sequentially followed by two distinct subpopulations of macrophages, which invade the injured muscle and become the predominant inflammatory cells (3,4). A highly orchestrated regeneration process follows the muscle degeneration stage. Upon exposure to signals from damaged environment, satellite cells exit their quiescent state and start proliferating. Activated satellite cells give rise to a transient amplifying population of myogenic precursor cells that undergo several rounds of division before migrating to the site of damage to enter terminal differentiation, fusing to existing damaged fibers or with one another to form *de novo* myofibers (1). Furthermore, satellite cells also possess the ability to undergo self-renewal to restock the quiescent satellite cell population, thus allowing tissue homeostasis and multiple rounds of regeneration during their life span (1). At molecular level, a broad spectrum of signals orchestrates the activation, proliferation and differentiation of the quiescent satellite cells. These signals include, among others, hepatocyte growth factor (5), insulin-like growth factors (6), myostatin (7), vasopressin (8) and Wnts (10). These signaling molecules determine the intracellular pathways that converge on a series of

transcription and chromatin-remodeling factors delineating the gene and microRNA expression program that delimit myogenic identity (1, 11). Myogenic transcription factors are organized in hierarchical gene expression networks that are spatiotemporally activated or inhibited during lineage progression (1, 12). In particular, the muscle regulatory factors (MRF), MyoD, Myf5, myogenin, and MRF4 are essential for myoblast lineage commitment. The MRF, in conjunction with other transcriptional regulators, induce the expression of muscle-specific genes, such as myosin heavy chain (MHC), that determine terminal myogenic differentiation (1, 12).

Much attention has been recently given to the understanding of the molecular and cellular mechanisms underlying skeletal muscle regeneration in different contexts, since such knowledge will ultimately facilitate the development of new treatments for myopathies (1, 11). One theoretical approach is the use of autocrine/paracrine signals in a therapeutic setting to help the replacement of damaged or degenerated muscle tissue. In this context, we have recently reported that obestatin, a 23-amino acid peptide derived from a polypeptide called preproghrelin, is involved in muscle regeneration, exerting an autocrine function to control the myogenic differentiation program (13). Obestatin is expressed in healthy skeletal muscle, and this expression is strikingly increased upon muscle injury. *In vitro*, obestatin is coordinately up-regulated during the early stages of myogenesis, and its level remains sustained throughout terminal differentiation. Functionally, blocking obestatin during myogenesis induces a decrease in myogenic-associated markers, such as myogenin and MHC, a process requiring the G protein-coupled receptor GPR39. Exogenous obestatin stimulation of undifferentiated myoblasts promotes the mitogenic activity and the migration function of myoblasts. Additionally, this peptide increases myogenic differentiation, leading to a rise of the fusion index. These results are endorsed by *in vivo* testing of skeletal muscles obtained from male rats under continuous subcutaneous infusion of obestatin. This peptide up-regulates of the hierarchy of transcription factors involved in the control of the different stages of the myogenic program: Pax7, Myf5, MyoD, myogenin and Myf6. Notably, obestatin increases the expression of

VEGF and its receptor isoform VEGFR2 for the potential regulation of the angiogenic process in skeletal muscle tissue. This latter effect is important for the potential regulation of the angiogenic process in the skeletal muscle providing the needed vascularization for developing skeletal muscle.

The ability of obestatin to drive different stages of the myogenic program suggests its potential use as a therapeutic agent for the treatment of trauma-induced muscle injuries or skeletal muscle myopathies. In the present study, we used an established model of skeletal muscle regeneration after injury to determine if obestatin, either by modulation of its expression or by exogenous administration, would enhance skeletal muscle regeneration after injury. Using several cellular strategies, we also analyzed the mitogenic and myogenic capabilities of this peptide and the associated-intracellular signaling pathways.

RESULTS

Overexpression of the obestatin/GPR39 system *in vivo* enhances muscle regeneration.

We previously demonstrated that GPR39 is required for the activation of obestatin signaling (13). To confirm that obestatin binds to GPR39, we performed a co-immunoprecipitation experiment using hemagglutinin (HA)-tagged obestatin (obestatin-HA). The HA tag does not interfere with obestatin bioactivity as evidenced by the increased phosphorylation of ERK1/2 and Akt in C2C12 myoblast cells (upper panel of Fig. 1a). As Fig. 1a (bottom panel) shows, obestatin-HA co-immunoprecipitated specifically with GPR39-GFP, but not with GFP alone. Thus, co-immunoprecipitation experiments demonstrated the binding of obestatin to GPR39 in cultured C2C12 myoblast cells. Therefore, we investigated the role of the obestatin/GPR39 system in muscle regeneration *in vivo*, preproghrelin, and thus obestatin, was overexpressed by electroporation of a CMV-preproghrelin expression plasmid into the TA muscles of 8-weeks-old mice. Freeze injury of the muscle was chosen due to the significantly reduced inflammatory response relative to other methods, such as cholera toxin injection. The changes

in protein expression were performed at 96-h post-injury, corresponding to the acute phase of regeneration, and at 168-h post-injury, when the satellite cells have returned to a quiescent stage. The histological analysis of the electroporated muscles with the CMV plasmid revealed no regeneration deficit as compared to control electroporations, where an empty vector was electroporated (Fig. 1b). In addition, the immunostaining of the TA muscles cryosections, 168-h following electroporation with the CMV plasmids, exhibited higher levels of preproghrelin, GPR39 or both (left panels of Fig. 1c and 2a-b, respectively). The CMV-preproghrelin electroporated TA muscles exhibited an increase in protein expression of Pax7, MyoD, myogenin and embryonic MHC (eMHC; Fig. 1c) at 96- and 168-h time points. At the same time points, overexpression of CMV-GPR39 plasmid also resulted in an increase of these myogenic markers (Fig. 2a). Notably, the electroporated TA muscles with both CMV-preproghrelin and CMV-GPR39 plasmid revealed a larger augment of Pax7, MyoD, myogenin and MHC (Fig. 2b) at 96- and 168-h time points. Taken together, these results indicate that overexpression of preproghrelin and/or GPR39 enhance muscle regeneration, as evidenced by the increase of the myogenic markers expression. Nonetheless, the electroporation conditions used also resulted in an injury to the muscle, raising the question of whether active regeneration is a direct consequence of the obestatin/GPR39 response.

Obestatin enhances muscle regeneration. To address whether the exogenous administration of obestatin is capable of stimulating effective regeneration, the dispersal of obestatin in tissue was assessed. Obestatin-HA (300 nmol/kg body-weight) was directly injected into the TA muscles of 2-month-old mice (n=5) and myofibers were visualized using immunostaining for the HA-tag present 30 min after administration (Fig. 3a). The proportion of HA-positive fibers in TA muscles ranged from 80 to 90% in distal zone from the injection site. Importantly, following intramuscular delivery, pAkt(S473) was present throughout the muscle and not purely localized at the injection site. The number of HA-positive fibers in the contralateral muscles from the HA-obestatin-treated mice (n = 5) did not show HA-

positive fibers ($\leq 1\%$), thus there was no evidence of significant systemic transfer of obestatin from the injected side (Fig. 3a). After the dispersal in tissue was evaluated, obestatin (300 nmol/kg body-weight) or vehicle (PBS) was directly injected into the TA muscles of 2-month-old mice ($n=35/\text{group}$) following freeze injury. The histological analysis (Fig. 3a) revealed that the treated-to-control ratios of regenerating fiber (i.e., with centrally located nuclei) cross-section areas were 62 and 28% larger in obestatin-treated mice (324 ± 29 and $755\pm 42 \mu\text{m}^2$) than in control mice (199 ± 22 and $588\pm 88 \mu\text{m}^2$) at 96- and 168-h after injury, respectively (Fig. 3c). At 240-h post-injury, cross-section area analysis revealed a significant increase, as compared to control, in the percentage of myofibers of larger area (Fig. 3d): 24% vs. 3% of fibers in a range between $4\text{-}3\times 10^3 \mu\text{m}^2$, 56% vs. 39% between $2\text{-}1\times 10^3 \mu\text{m}^2$, and 18% vs. 56% between $1\text{-}0.5\times 10^3 \mu\text{m}^2$. This pronounced increase of regenerating in obestatin-treated muscle was concomitant with significant increases, as compared to control, in the protein expression of Pax7, MyoD, myogenin and eMHC for the time tested (Fig. 3e-i). To confirm the eMHC up-regulation during muscle regeneration, immunofluorescence analyses were performed on cryosections of freeze-injured TA fixed 96-h post-injury (Fig. 3j). In the control TA-muscle, eMHC was expressed at detectable levels in regenerating fibers, of smaller size than the intact fibers (Fig. 3j, left). By contrast, eMHC was markedly up-regulated in the obestatin-treated TA muscles (Fig. 3j, right). The number of myonuclei per myofiber was significantly increased by 91% in the obestatin-treated (481 ± 19 cells per muscle section) compared to the control TA muscles (251 ± 17 cells per muscle section) at 240-h after injury (Fig. 4a). Furthermore, we analyzed the serum levels of creatine kinase (CK), a skeletal muscle enzyme released during fiber degeneration (14), at 96-h post-injury. In this time-window, treatment with obestatin reduced the CK levels with respect to those observed in untreated injured-control animals, suggesting a decrease in the level and severity of muscle damage (Fig. 3k). Taken together, these data demonstrate that obestatin delivered by intramuscular injection markedly enhances regenerative capacity, as achieved by up-regulation of the expression of specific myogenic factors, the significantly increased size of the

regenerating myofibers, the muscle fiber growth, the increased myonuclei addition, and the decreased serum CK levels.

Obestatin enhances satellite cell activation after muscle injury. Based on the up-regulation of Pax7 expression, a specific satellite cells marker (1), in the obestatin-treated TA muscles, satellite cells were quantitated in TA muscle sections 96-h post-injury (Fig. 4b). The satellite cells density in the obestatin-treated TA muscles harbored ~2.3-fold more Pax7⁺ cells per section (427 ± 7 cells per muscle section) than the control TA muscles (189 ± 12 cells per muscle section) at 96-h after injury. In addition, satellite cell number normalized to myofiber length (myofibers isolated from the neighboring area of the injured zone) harbored 2.2-fold more Pax7⁺ cells in the myofibers obtained from the obestatin-treated than in the control muscles (Fig. 4c). The elevated number of the Pax7⁺ cells implies that satellite cells underwent enhanced proliferation during muscle regeneration. To ascertain this possibility, the expression of Ki67 and Cyclin D1 was evaluated at 96-h after injury. The elevated protein level of Ki67, 2.3-fold higher in the obestatin-treated than in the control TA muscles (Fig. 5a), implies an enhanced proliferation at 96-h after muscle injury. Added to this fact, the elevated protein expression of Cyclin D1, 2.2-fold higher in obestatin-treated than in control TA muscles, demonstrated enhanced proliferation during regeneration (Fig. 5b). Taken together, these data demonstrated that obestatin enhances satellite cell proliferation during the early stages of muscle regeneration.

Muscle force analysis. Present results demonstrated that obestatin induced repair and growth by stimulating both satellite cell expansion and myofiber hypertrophy. An unanswered question was whether or not the obestatin-treated muscles generate higher specific forces than control muscles under this protocol. To address this question, the force generated by TA muscles from obestatin-treated mice was measured. Mean twitch and tetanic force of normal TA were respectively 0.21 and 1.36 N (Fig. 5a and b, respectively). Mean twitch and tetanic force were fewer 10 days after the induction of injury as

the means were 0.16 and 0.94 N, representing a 24 and 34% loss of force, respectively. However, despite an improvement of fiber regeneration with obestatin, no difference in mean twitch and tetanic force was observed between vehicle- and obestatin-treated TA. The lack of a better functional recovery with obestatin suggests that functional recovery takes longer than 10 days, or more likely that by 10 days the neuromuscular junctions are still not fully functional and this is important because TA contractions were elicited by stimulating the peroneal nerve.

Obestatin affects the essential network for regenerating muscle fiber growth. The obestatin-treated-to-control ratios of VEGF and VEGF-R2 protein levels were 130 and 80% higher in obestatin-treated than in control TA muscles at 96-h after injury, respectively (Fig. 6c and d). The vessel counting, evaluated as isolectin⁺ per myofiber, showed differences in capillary density in the obestatin-treated (1.5 ± 0.06) compared to control TA muscles (0.5 ± 0.01) at 96-h post-injury (Fig. 6e). These data indicated that obestatin contributed to the restoration of the VEGF/VEGF-R2 tissue levels. Of note, there was no significant elevation of collagen 1 α 2 (Col1 α 2) in obestatin-treated TA muscles at 96-h and 240-h after injury (Fig. 6f, upper panel). This result was supported by Heidenhain's AZAN trichrome staining of the muscle sections 240-h after injury (Fig. 6f, lower panel). This fact indicated that fibrosis is not enhanced during regeneration in the obestatin-treated muscles and did not contribute to the increased size of the regenerated muscle. On the other hand, the myostatin protein levels, measured as the precursor latency-associated peptide (LAP) and dimer, were respectively 20, 30 and 60% lower in the obestatin-treated than in the control TA muscles at 96-h after injury (Fig. 6g), which corroborated the obestatin role on muscle regeneration and growth.

Obestatin enhances myogenic cell proliferation. Obestatin showed a marked enhancement of the regeneration process, an effect probably dependent on myoblast proliferation or differentiation. To ascertain this possibility, the mitogenic action of obestatin was explored by dose-effect experiments

performed on cultured C2C12 myoblasts treated with a range of obestatin concentrations (0.1–100 nM) in GM (proliferating conditions; Fig. 7a). The maximal effect in the cell number was observed at 5 nM obestatin (~2.4-fold). During the differentiation process, the immunoblot analysis of Ki67, p57 and p21 revealed elevated protein expression when compared the obestatin-treated cells (DM+5 nM obestatin) with the control cells (DM; Fig. 7b). At 24-h, Ki67 showed maximal expression levels, followed by an increase in the expression of p57 and p21, reflecting growth arrest to promote cellular differentiation. In fact, the protein levels of myogenin and MHC were up-regulated, displaying maximal levels at 72- and 96-h respectively (Fig. 7b). Of note, both proliferating and myogenic markers displayed normal kinetics with enhanced protein levels when compared the obestatin-treated with the control cells.

Obestatin enhances myoblast fusion and hypertrophic growth of myotubes. The exogenous administration of obestatin to TA during regeneration enhanced the area and the number of myonuclei per myofiber. To investigate whether obestatin in fact stimulated hypertrophic growth, the C2C12 myoblasts were first treated with obestatin under DM (Fig. 8a). The myotube areas were 110% larger in the obestatin-treated cells (DM+5 nM obestatin; $941 \pm 4 \mu\text{m}^2$) than in the control cells (DM; $449 \pm 3 \mu\text{m}^2$) at 168-h after differentiation. Moreover, the myotubes were grouped into two categories, those with 3 myonuclei and those with 4 or more myonuclei. ~30% of the control myotubes contained 4 nuclei *versus* the 73% of the obestatin-treated cells. This effect represents an increase of ~1.93-fold respect to the control cells (Fig. 8a). Having shown that obestatin induced hypertrophy with enhanced nuclei addition, we assessed whether the administration of obestatin 3 days after the initiation of differentiation was responsive to obestatin-induced hypertrophy in culture (Fig. 8b). In this case, the myotube areas were ~80% larger in the obestatin-treated cells (DM for 72-h followed by DM+5 nM obestatin for 96-h; $736 \pm 7 \mu\text{m}^2$) than in the control cells (DM; $409 \pm 6 \mu\text{m}^2$) at 168-h after differentiation. Under these conditions, ~40% of the control myotubes contained 4 nuclei *versus* the 87% of the

obestatin-treated cells. Furthermore, the myotubes were treated with obestatin after administration of cytosine arabinoside (AraC), an inhibitor of DNA replication to abolish the *de novo* fusion of the myoblasts (15). Of note, the obestatin-treated cells displayed ~92% larger myotubes areas (DM for 72-h followed by DM+AraC (50 μ M)+obestatin (5 nM) for 96-h; $853\pm 3 \mu\text{m}^2$; Fig. 8c) than in the control cells (DM; $444\pm 4 \mu\text{m}^2$) at 168-h. Obestatin treatment led to a ~75% of myotubes containing 4 nuclei *versus* the 33% in the control cells. The immunoblot analyses revealed no differences in myogenin and MHC levels between both groups: DM+obestatin and DM+AraC+obestatin (Fig. 8d). Taken together, these data showed that obestatin exerted a bidirectional role within the myotube, controlling the myoblast recruitment to fuse and the growing volume.

Obestatin controls myogenesis by regulating Akt, ERK1/2, p38 and CAMKII activity. To establish the molecular events activated by obestatin to drive the myogenic process, the activity of Akt/mTOR signaling was analyzed in differentiating C2C12 cells during 168-h (Fig. 9a). The obestatin treatment (5 nM) resulted in markedly elevated levels of phosphorylated Akt [pAkt(S473)] and its downstream target S6K1 [pS6K1(S371)] during the myogenesis. Despite the increased Akt activity under the obestatin treatment, lower levels of pFoxO1(T24) and pFoxO3a(T32) observed in the obestatin-treated cells than in the control cells (DM). Obestatin increased ERK1/2 activity [pERK1/2(T202/Y204)] in the early steps of the differentiation program. Strikingly, obestatin markedly elevated the levels of phosphorylated p38 [pp38(T180/Y182)] during the differentiation. The phosphorylation levels of c-Jun [pc-Jun(S63)] showed no significant differences following the obestatin treatment compared to the control cells. By contrast, the phosphorylation pattern of CAMKII [pCAMKII(T286)] showed clear differences under the obestatin treatment. A gradual increase of pCAMKII(T286) was observed in the control cells, reaching maximal levels at 168-h. Under obestatin treatment, the maximal level was showed at earlier time points, 12-48 h, to decline to basal phosphorylation after 48-h. In regenerating TA muscle, obestatin treatment resulted in a robust

activation of Akt and S6K1 at 96-h after injury (Fig. 10a). Other signaling components, ERK1/2, FoxO1, FoxO3a, p38, c-Jun and CAMKII, did not show significant differences in phosphorylation at this time point. Together, a kinase hierarchy determined the action of obestatin in an analogous manner to the myogenic transcription factors.

Obestatin regulates myogenesis by limiting IGFR/IRS1 activity. Obestatin signals to activate the Akt/mTOR pathway through cross-talk with tyrosine kinase receptors, i.e. EGFR (16). To investigate the possibility that obestatin was indirectly activating the Akt/mTOR pathway through IGFR, the activation of IFGR [measured as pIGFR(Y1316)], was examined in differentiating C2C12 cells during 168-h (Fig. 8b). Obestatin showed to increase the level of pIGFR(Y1316) at early time points (12-48-h). However, under these conditions there was a substantial increase of the IRS-1 phosphorylation at S636/639 [pIRS-1(S636/639)], sites shown to inhibit PI3K binding to IRS-1 and consequent activation of Akt-associated IGFR signaling (Fig. 9b) (17). In regenerating TA muscle, obestatin treatment showed to enhance the levels of pIGFR(Y1316) and pIRS-1(S636/639) at 96-h after injury (Fig. 10b). Therefore, obestatin action on Akt/mTOR pathway is independent of IGFR/IRS1 activity.

DISCUSSION

The principal finding of this study is that obestatin increases muscle regeneration after skeletal muscle injury. Our results have evidenced that: 1) the overexpression of the obestatin/GPR39 system in skeletal muscle enhanced muscle regeneration after muscle injury; 2) the intramuscular injection markedly enhances muscle regeneration, as evidenced by the up-regulation of the expression of the specific myogenic factors (Pax7, MyoD, myogenin) and eMHC, the noteworthy decrease of serum CK levels, and, more importantly, the significant increase of the myofiber size and the number of myonuclei per myofiber; 3) the up-regulation of the specific satellite cells marker Pax7, associated to the increased

number of activated satellite cells (Pax7⁺) per myofiber, demonstrated the actions of obestatin on satellite cells; 4) the effective action was due to a specific regulation of this peptide on the different stages affecting the myogenesis: proliferation, migration, fusion and myofiber growth; 5) added to the myogenic action, obestatin administration resulted in an increased expression of VEGF/VEGFR2 and microvascularization, with no significant effect on collagen deposition in developing skeletal muscle; 6) the potential inhibition of myostatin might contribute to the myogenic action improving muscle growth and regeneration; and, 7) the myogenic actions of obestatin were coordinated by a kinase hierarchy determined by the ERK1/2, CAMKII, Akt and p38 axis. These findings unveil a role for obestatin in the regulation of satellite cell-mediated muscle regeneration and identify obestatin as a potential therapeutic target for a variety of conditions related to muscle regeneration.

In response to obestatin, the hierarchy of transcription factors regulating progression through the myogenic lineage was clearly increased. This is endorsed by the increased expression of myogenic regulator factors, Pax-7, MyoD, and myogenin, demonstrating the myogenic potential for this peptide when it is administrated into injured muscle. The up-regulation of Pax7 expression is indicative of a control on satellite cell activation to enhance myogenic specification and/or to induce self-renewal (18). It is known that this transcription factor is maintained in satellite cells and proliferating myoblasts but it is down-regulated before differentiation (1, 19). Indeed, satellite cell number increased on muscle sections as well as in myofibers obtained from obestatin-treated muscles at 96-h after injury. The increased satellite cell proliferation was concomitant with an enhanced tissue expression of Ki67, a proliferating cell marker, and Cyclin D1, a well-known effector of the G1 to S cell cycle phase transition, at 96-h after injury, although it does not exclude the implication of any other cell type that is proliferating. Added to the increasing Pax-7 expression level, obestatin-treated mice showed up-regulation of MyoD expression. MyoD is an important determinant of myogenic differentiation, although MyoD expression does not always ensure myogenic commitment. It was found that the ratio of

Pax7/MyoD activities becomes critical for the control of satellite cell fate (reviewed in 1). However, the induction of myogenin expression, which primarily depends on MyoD (1), denoted the initiation of terminal differentiation. This program dictates the differentiation process driving the transformation from individual proliferating myogenic cells to myofibers. This transition was supported by the up-regulation of proteins such as MHC. Further support was demonstrated by the augmentation of the myogenic markers by *in vivo* overexpression of preproghrelin during muscle regeneration. However, it would implicate the contribution of the preproghrelin-derived peptides, ghrelin, des-acyl ghrelin and obestatin (13, 20, 21), as pro-myogenic signals. Overexpression of GPR39 resulted in up-regulation of the myogenic cascade, a result that supports the autocrine role of obestatin to trigger the myogenic differentiation program (13). Importantly, *in vivo* co-overexpression of GPR39 and preproghrelin during muscle regeneration resulted in a larger enhancement of the myogenic markers compared to that obtained from GPR39 or preproghrelin overexpression alone. These findings emphasize the remarkable role of the obestatin/GPR39 system into the remodeling of damaged fibers following injury. It should be highlighted that despite electro-transfer of DNA demonstrated to be an efficient method to deliver genes, the results could be improved by viral gene transfer whose effectiveness is clearly superior.

At late stage of muscle regeneration, obestatin treatment increased the cross-sectional area of the newly formed muscle fibers. Another effect of obestatin favoring muscle regeneration was the increased density of myonuclei in regenerating fibers. This duality might be interpreted as a result of mitotic expansion of satellite cells to differentiate and repair the tissue reestablishing homeostasis. Given that myonuclei are post-mitotic, the necessity of expansion of committed satellite cells, myoblasts, for muscle hypertrophy was determined under obestatin stimulation 3-days after C2C12 differentiation, or in AraC-treated cultures. Under these conditions, the growth response and myonuclei accretion induced by obestatin was not altered. Furthermore, the protein expression of myogenin and MHC was not affected by AraC treatment. Thus, the hypertrophic response to obestatin was not associated with the

addition of new myonuclei *via* proliferation and further fusion. Added to this fact, immunoblot analyses revealed normal, although enhanced, kinetics of myogenin or MHC expression ruling out accelerated kinetics of the differentiation program. This scenario proposes that the hypertrophy or fusion response to obestatin is not consequence of accelerated kinetics of differentiation or enhanced myoblast proliferation. The result that hypertrophy response was independent of myoblast proliferation is not without precedent. Specifically, it was reported that hypertrophy resulting from Wnt7a stimulation occurred without the enhancement of myoblast proliferation or accelerated kinetic of differentiation (15). It should be considered that hypertrophy is strongly associated to the level of Akt/mTOR/S6K1 activation, a pathway activated by obestatin during the differentiation program and the diverse stages comprised in the process of skeletal muscle regeneration (22, 23). This pathway controls mechanisms of protein synthesis at several stages (e.g., translation capacity, translation efficiency) through the increase of specific mRNAs translation, which results in myotubes and fiber enlargement.

In addition to its myogenic action, obestatin also regulated the expression of factors that define the regenerative microenvironment responsible for stimulating and coordinating skeletal muscle repair. In this sense, obestatin increased the expression of VEGF and its receptor isoform VEGF-R2 during muscle regeneration. Besides being described as a myogenic factor (24), VEGF was shown to stimulate muscle healing by promoting angiogenesis (25, 26). Precisely, the VEGF produced by differentiating myocyte provides the needed vascularization for the developing skeletal muscle. Our results further indicated that obestatin-treated injured muscles increased capillary density being indicative of enhanced microvascularization. These new developed capillaries sprout out from peripheral surviving capillaries, helping to provide the injured area with oxygen and substrates aiding in the regenerative process. Added to vascularization, obestatin reduced the expression of myostatin, a highly conserved transforming growth factor- β family member (27). Myostatin regulates muscle growth through a direct inhibition of the proliferation and differentiation of the satellite cells (28, 29). Although myostatin inhibits myocyte

proliferation and differentiation, it regulates muscle fibrosis through the stimulation of muscle fibroblasts and the expression of extracellular matrix proteins, such as collagen (30, 31). In this sense, it is important to note that obestatin treatment did not increase collagen deposition in regenerating muscle ruling out a fibrotic response. Whereas obestatin directly stimulates myogenesis, it is logical to postulate that this effect might be mediated partially through inhibition of myostatin. Furthermore exists the possibility that the inhibition of myostatin contributes to the regulation of extracellular matrix proteins. This is supported by the finding that myostatin stimulates collagen production of muscle fibroblasts (31). Thus obestatin regulates the new vessel formation and/or remodeling of the preexisting vasculature under the control of local pro-angiogenic program, such as VEGF/VEGFR2 system, representing an integral component of muscle tissue remodeling which control the extent of the injury preventing a deleterious microenvironment characterized by fibrosis.

One of the most remarkable observations from this study was that obestatin has multiple functional properties associated to the skeletal muscle regeneration, and its capability to stimulate proliferation, differentiation, fusion and hypertrophy response is under regulation of a kinase hierarchy. The cell cycle arrest and the onset of differentiation are orchestrated by p21 and p57. In our study, the expression of p57 and p21 is linked to an absence of cell cycle progression, since we observe no overlap with Ki67. MyoD has been suggested to be a direct regulator of *p21*, thus controlling the cell cycle exit during adult muscle differentiation (32). It has also been shown that p57 interacts and stabilizes MyoD to promote muscle differentiation (33, 34). In this way, interactions between cyclin-dependent kinase inhibitors essential for myogenic growth and MRFs orchestrate the proliferation, specification and differentiation of muscle progenitor cells (35, 36). In the C2C12 differentiating myoblasts, obestatin enhanced ERK, CAMKII, Akt, and p38 activities. These pathways displayed the ability to execute different stages of the regeneration program. On one side, ERK1/2 belongs to a well-defined pathway, which is critical for cellular proliferation and migration (37). In the context of obestatin-induced activity, ERK initially

decreased with myoblast differentiation, which is necessary for differentiating myoblasts to overcome its inhibitory effect. Indeed, ERK was shown to inhibit differentiation by preventing the nuclear accumulation of members of the myocyte enhancer factor-2 (38), and the expression of certain myogenic factors, including MyoD (39) and the CDK inhibitor p21 (40). In the case of CAMKII, its signaling prevents the formation of MEF2–HDAC complexes by phosphorylation of HDAC4/HDAC5, promoting a nuclear export of these transcriptional repressors and the rising of MEF2 activity on muscle specific genes such as MyoD and myogenin (41). In particular, the earlier activation of CAMKII by obestatin (≥ 12 -h) compared with that of control (≥ 144 h), is not consistent with a premature expression of myogenin in response to obestatin compared with control. This piece of information reveals additional roles for CAMKII in the obestatin-regulated signaling during differentiation. Thus it is possible to speculate about the role of this kinase in the regulation of cell cycle, and hence, the control of the proliferative step during differentiation, based on its function on G2/M and the metaphase-anaphase transition described for it (42). Regarding the Akt pathway, this route has emerged as a critical signaling node within myogenic program. The consequences of Akt activation include diverse responses, ranging from primarily metabolic functions such as glucose transport, glycolysis, glycogen synthesis, and the suppression of gluconeogenesis to protein synthesis, increased cell size, cell-cycle progression and apoptosis suppression (43). Obestatin showed to increase the levels of activated Akt during myogenesis. The wide range of cellular functions mediated by this kinase is related to the different Akt isoforms. Thus, Akt1 was described to be essential in early differentiation leading to cell cycle progression (44). By contrast, Akt2 triggers myoblast cell cycle exit and drives differentiation determining myotube maturation (44). Following to the commitment in the myogenic differentiation, the hypertrophic muscle growth induced by obestatin might be under the regulation of the downstream effectors of the Akt pathway, FoxO1 and FoxO3a (22, 45, 46). However, the degree of obestatin-induced phosphorylation of FoxO1 and FoxO3a remained lower than in the untreated cells, pointing to a pivotal role for the S6K1-dependent pathway. p38 kinase activity increased over the course of differentiation under obestatin

treatment, a fact that fit well with the established role of this kinase in the cell cycle arrest and full myoblasts differentiation through the control of muscle-specific gene expression (47, 48). Our results further showed that obestatin mediated the cessation of the JNK/cJun proliferation-promoting pathway, prerequisite for the commencement of the differentiation program (49). Interestingly, decreased activation of the JNK/cJun pathway was concomitant to p38 activation in differentiation-promoting conditions under obestatin treatment. The convergence of these pathways at the chromatin level defines the mechanism for integration of mitogenic and myogenic signals to direct the transition from quiescence to terminal differentiation (50). Therefore, obestatin action is a highly coordinated process in which various signaling pathways converge to activate a specific gene expression program associated to each stage of the myofiber formation process.

Once obestatin activates GPR39, two routes are triggered in parallel: 1) sequential activation of G_i , PI3K, novel PKC ϵ and Src and the subsequent ERK1/2 activation; and 2) a β -arrestin 1-mediated signaling pathway that involves the recruitment of Src to the β -arrestin 1 scaffolding complex, and thus Akt phosphorylation (16, 51). In this way, Akt activation is switched by cross-activation of receptor tyrosine kinases, i.e. EGFR, in which Src acts to activate matrix metalloproteinases to initiate the proteolytic release of the EGF-like ligands onto the cell surface, which later bind to EGFR. Based on this cross-activity, one might wonder whether obestatin-associated Akt activity, such as skeletal muscle hypertrophy, might simply be switched by cross-activation of IGFR, one of the main regulators of muscle mass by stimulating the Akt/mTOR pathway (22). Indeed, obestatin transactivated IGFR, a process that leads to activation of Akt by stimulating the IRS-1/PI3K pathway. Interestingly, there was a substantial increase of the IRS-1 phosphorylation at S636/639, sites shown to inhibit PI3K binding to IRS-1 (17) and thus the Akt/mTOR signaling associated to IGFR. At present, it is well documented that S6K1 is implicated in a negative feedback loop on IRS-1 S636/639 phosphorylation to suppress PI3K signaling (17, 52, 53). Consistent with this finding, our results showed that the increase of pS6K1(T389)

levels paralleled to the enhancement in pIRS-1(S636/639). Under these conditions, the S6K1 activation impaired IRS-1/PI3K signaling decreasing the Akt associated signaling to IGFR. Despite the cross-activation of IGFR, the negative feedback loop from S6K1 to IRS-1 rules out the implication of IGFR/IRS-1 system in the obestatin-induced Akt/mTOR signaling. Therefore, obestatin-associated Akt kinase activity, i.e. myogenesis or muscle growth, is independent of IGFR/IRS1 pathway.

In summary, our findings provide compelling evidence for the use of obestatin as a therapeutic approach to stimulate muscle regeneration. On a first consideration, the current study raises the possibility of a new strategy for skeletal muscle repair by local administration into the injured site. It is important to note that sports-related injuries can pose challenging problems in sport medicine and traumatology. The best treatment for the most common acute muscle injuries has not been clearly defined yet, and the recommended treatment regimens are mostly conservative and routine. Additionally, to develop superior treatments for treating muscle pathologies, an interesting area has arisen focusing on the modulation of satellite cells function through the identification of autocrine factors and the related molecular pathways that govern their activation and proper differentiation. The ability of the obestatin/GPR39 system to activate stem cell expansion and muscle growth combined to its role on vascularization and fibrosis makes obestatin a promising candidate, if it has no deleterious side effect, Ideally, this type of therapy would activate satellite cells to enhance their regenerative potential avoiding the exhaustion of such cells. Although this mode of action does not treat the genetic basis of the pathological background associated to some of the muscle pathologies, it might be sufficient to maintain a stable level of regeneration and reduce the severity of certain symptoms. Furthermore, endogenous repairing factors are also required for combinatorial therapies with gene or cell-based strategies. Thus, future investigations in the development of these simple therapeutic approaches, targeting satellite cells, can offer new and important possibilities for the amelioration of skeletal muscle diseases.

MATERIALS AND METHODS

Materials. Rat/mouse obestatin was obtained from California Peptide Research (Napa, CA, USA). Hemagglutinin (HA)-tagged obestatin (obestatin-HA) was obtained from Biomedal (Sevilla, ES). Antibodies used are listed in Table S1. All other chemical reagents were from Sigma Chemical Co. (St. Louis, MO, US).

Mice and animal care. This study used 8-weeks-old female Swiss mice (30 g). Mice were housed in 12 hours light/12 hours dark cycles with free access to standard mice chow diet and water. All mice were maintained inside animal care facility and the experiments were performed in accordance with University of Sapienza (Rome, Italy) and University of Santiago de Compostela (Santiago de Compostela, Spain) guidelines for animal handling and care. For the experiments at the University of Ottawa (Ottawa, Canada), all procedures were approved by the Animal Care Committee of the University of Ottawa according to guidelines of the Canadian Council for Animal Care (CCAC).

Freeze-induced muscle injury and obestatin dosing. The experimental protocol used in the present work was previously optimized and validated by Moressi V et al. (14). Under anesthesia, the hindlimbs of the mice were shaved and both tibialis anterior muscles (TA) were exposed via a 1-cm-long incision in aseptically prepared skin overlying the muscle. Traumatic freeze injury was induced by applying a 120-mm-diameter steel probe, pre-cooled to the temperature of dry ice (-79°C), to the belly of the TA muscle for 10 seconds. After injury procedure, the skin incision was closed using 6-0 silk sutures. This procedure induced a focal injury extending distally from the spike of the tibia and spreading over approximately one-third of the muscle. The average length and maximal cross-sectional area of the lesion sites, evaluated by Evans Blue labeling (14), were $3202 \pm 14 \mu\text{m}$ and $3875789 \pm 27501 \mu\text{m}^2$, respectively (mean \pm SEM). Animals were assigned to one of two-matched experimental groups

(n=35 per group): 1) Obestatin-treated group; and, 2) control group. Obestatin treatment was performed via injection of 20 μ L of obestatin solution in PBS [300 nmol/kg body weight (13)] into the target muscles each 24 hours (h) during 5 days. Control group was treated with 20 μ L of PBS under same conditions. Injections were performed twice per muscle inserting the needle of a 0.3 mL/29 gauge syringe (Becton, Dickinson and Company, Franklin Lakes, NJ) for 1 mm in the distal part of the muscle, in a region that is not taken into account for histological analysis, as it was previously demonstrated (14). This procedure did not induce muscle fiber damage, as Evans Blue uptake was not detectable following injection in an adult muscle. TA muscles from both groups were excised at indicated time points (12-240 hours; n=5 per time point) and processed for immunoblot, immunohistochemistry and/or immunofluorescence analyses.

In vivo electroporation. To overexpress preproghrelin and/or GPR39 [mouse preproghrelin (GenBank NM_021488.4) and GPR39 (GenBank NM_027677) cDNAs in pCMV6-entry vector were from OriGene Tech (Maryland, USA)], the plasmid DNAs or pCMV6 (Mock; Origene; MD, USA) in PBS were directly co-injected with 5 μ g pcDNA 3.1-SNAP-GFP (transfection marker; kindly provided by Prof. Pozzan; University of Ferrara, Italy) into TA of 8-weeks-old female Swiss mice (30 g) followed by electroporation. Electroporation was performed before muscle injury by delivering six electric pulses of 20 V each (three with the anode placed on the front of the TA, followed by three pulses with inverted polarity). A pair of 3 \times 5 mm Genepaddle electrodes (BTX, San Diego, CA) placed on each side of the TA muscle was used. The electrodes cover an area corresponding to the majority of the muscle surface and, thus, totally overhang the area of injury. This protocol of gene delivery by electroporation guarantees stable DNA expression for more than 4 months (8). Mice were sacrificed at 96- and 168-h (n=5 per group) after injury.

Myofiber isolation. Single myofibers were isolated from TA muscles as previously described (54). For *in vivo* activation of satellite cells, regeneration was induced in the TA after freeze injury and individual myofibers were isolated 96-h later from the neighboring area of the injured zone of the TA muscle. Immunochemical labeling of myofibers were performed as previously reported (55).

Force measurement. Mice were anaesthetized by intraperitoneal injection of 2.2 mg ketamine/0.4 mg xylazine/ 0.22 mg acepromazine per 10 g of animal body weight. Mice were put on a heating pad to maintain body and muscles at 37°C. The distal tendon of the TA muscle was attached to a FT03 Grass Instruments force transducer, which was connected to a Grass physiograph (Model 79D, Grass Technologies, Warwick, USA). An output of the polygraph was also connected to a digital data acquisition system (KCPI3104, Keithley, USA) to acquire force at a sampling rate of 5 kHz. TA was kept moist with a physiological solution containing 118.5 mM NaCl, 4.7 mM KCl, 1.3 mM CaCl₂, 3.1 mM MgCl₂, 25 mM NaHCO₃, 2 mM NaH₂PO₄, and 5.5 mM D-glucose continuously gassed with a mixture of O₂:CO₂ (95:5) to maintain a pH=7.4. Contractions were evoked every 100 sec by field stimulation using two platinum wires 0.6 cm apart on a short section of the peroneal nerve. The platinum electrodes were connected to a Grass S88X stimulator and a Grass SIUV isolation unit (Grass Technologies, Warwick, USA). Single twitches were elicited with one 0.3 msec square pulse at 10 V. Maximum force was measured during a tetanic contraction with 200 msec train of pulses at 200 Hz.

Cell culture and differentiation. Mouse C2C12 myoblasts were cultured as described by the supplier (ECACC, Whiltshire, UK). Briefly, the C2C12 myoblasts were maintained in growth medium (GM) containing DMEM supplemented with 10% fetal bovine serum (FBS), 100 U/mL penicillin, and 100 U/mL streptomycin. For routine differentiation, the cells were grown to 80% confluence and GM was replaced with differentiation medium (DM; DMEM supplemented with 2% FBS, 100 U/mL penicillin, and 100 U/mL streptomycin) for 7 days unless otherwise stated.

Cell transfection and co-immunoprecipitation. To overexpress GPR39 (GFP-tagged) [mouse GPR39 cDNAs in pCMV6-AC-GFP was from OriGene Tech (Maryland, USA)], the plasmid DNA or pCMV6-AC-GFP (Mock; Origene; MD, USA) were transfected in C2C12 myoblast cells using Lipofectomine 2000 according to instructions provided by the manufacturer. The relative percentage of GPR39-GFP transfection, expressed as % GFP-positive cells, was $70\pm 7\%$. Obestatin-HA, obtained from Biomedal (Sevilla, ES), was administered to the cells in a final concentration of 5 nM for 2 min. Co-immunoprecipitation was conducted using Chromotek-GFP Trap beads purchased from Allele Biotechnology&Pharmaceuticals according to instruction provided by manufacturer.

Histology and immunofluorescence. Muscle samples were mounted in tissue freezing medium (tragacanth paste) and snap frozen in nitrogen-cooled isopentane. The sections, 10 μm thick, were mounted on Histobond Adhesion Microslides (Marienfeld, Lauda-Königshofen, DE). For the haematoxiline/eosin and Heidenhain's AZAN trichrome stains, serial cryostat sections were stained following a standard protocol. Muscle sections for immunofluorescence analysis were permeabilized and blocked with PBT [1% Triton X-100, 1% Tween-20, 5% heat inactivated goat serum, 0.2% BSA in PBS] for 30 min, and incubated with primary antibodies diluted in PBT overnight at 4°C, washed with PBS and then incubated with a mixture of appropriate secondary antibodies for 45 min at 37°C. DAPI was used to counterstain the cell nuclei (Life Technologies, Invitrogen, Gran Island, NY, US). For quantification of regenerating fibers, identified by morphological criteria (i.e. centrally located nuclei), and myofiber cross-section area, the cryostat sections were stained with haematoxylin/eosin and five randomly chosen microscopic fields from two different sections in each tissue block were examined using ImageJ64 analysis software. Quantification of satellite cells in a whole section of TA muscles was performed by counting Pax7 positive cells (Pax7⁺) using ImageJ64 analysis software. At least 4 sections from each TA muscle were analyzed and the mean results of sections from each muscle were further

calculated as mean value of muscles. Quantification of satellite cells, based on single myofibers, was performed by quantitating Pax7⁺ cells in at least 12 myofibers isolated from the neighboring area of the injured zone of the TA muscle. For vessel counting, the total number of isolectin⁺ vessels neighboring and the total number of laminin myofibers were measured for each cross-section. For analysis of cultured cells, the C2C12 cells were cultured on coverslips and differentiated into myotubes. The intact cells were fixed with 4% buffered paraformaldehyde-PBS, washed, permeabilized and blocked with PBT, and then stained with primary antibody diluted in PBT overnight at 4°C. The cells were then washed and incubated with secondary antibody for 45 min at 37°C. DAPI was used to counterstain the cell nuclei (Life Technologies, Invitrogen, Gran Island, NY, US). Five fields from three independent experiments were randomly selected for each treatment. The differentiation grade was evaluated based on the number of MHC positive cells above total nuclei. The number of nuclei within individual myotubes (≥ 2 nuclei) was counted for 20–50 myotubes. The myotubes were grouped into two categories, those with 2 to 3 nuclei and those with 4 or more nuclei, and the percentage of the myotubes in each category was calculated relative to the untreated cells (20). The digital images of the cell cultures were acquired with a Leica TCS-SP5 spectral confocal microscope (Leica Microsystems, Heidelberg, DE).

Immunoblot analysis. The tissue or the cell samples were directly lysed in ice-cold RIPA buffer [50 mM Tris-HCl (pH 7.2), 150 mM NaCl, 1 mM EDTA, 1% (v/v) NP-40, 0.25% (w/v) Na-deoxycholate, protease inhibitor cocktail (Sigma Chemical Co, St. Louis, MO, US), phosphatase inhibitor cocktail (Sigma Chemical Co, St. Louis, MO, US)]. The lysates were clarified by centrifugation (14,000xg for 15 min at 4°C) and the protein concentration was quantified using the QuantiProTM BCA assay kit (Sigma Chemical Co, St. Louis, MO, US). For immunoblotting, equal amounts of protein were fractionated by SDS-PAGE and transferred onto nitrocellulose membranes. Immunoreactive bands were detected by

enhanced chemiluminescence (Pierce ECL Western Blotting Substrate; Thermo Fisher Scientific, Pierce, Rockford, IL, US).

Creatine kinase activity assay. Serum creatine kinase was assayed using the Enzy-Chrom Creatine Kinase Assay Kit (BioAssay Systems) according to the manufacture's instructions.

Data analysis. All values are presented as mean \pm standard error of the mean (SEM). Student *t* test were performed to assess the statistical significance of 2-way analysis. For multiple comparisons, ANOVA was employed. $P < 0.05$ was considered as statistically significant (*).

ACKNOWLEDGMENTS

This work was supported by grants from Instituto de Salud Carlos III (ISCIII; Ministerio de Economía y Competitividad, Spain; PS12/02388), Ministerio de Economía y Competitividad (SAF2010-20451, RYC-2008-02219 and BFU2012-35255), Xunta de Galicia (EM 2012/039), Fundación Mutua Madrileña and Asociación Duchenne Parent Project España. This work was partially supported by MIUR through PRIN project 2009WBFZYM_001, and by the Sapienza University of Rome Research Project C26A125ENW, both to S.A. Funders had no role in study design, data collection and analysis, decision to publish or preparation of the manuscript. Marta Picado Barreiro for assistance with the confocal microscope experiments. The work of JP Camina and Y Pazos are funded by the ISCIII and SERGAS through a research-staff stabilization contract. U Gurriarán-Rodríguez and J González-Sánchez were funded by Xunta de Galicia through a research-staff contract Isabel Barreto and pre-doctorate research scholarship, respectively.

REFERENCES

1. Yin H, Price F, Rudnicki MA (2013) Satellite cells and the muscle stem cell niche. *Physiol Rev* **93**: 23-67
2. Tidball JG, Villalta SA (2010) Regulatory interactions between muscle and the immune system during muscle regeneration. *Am J Physiol Regul Integr Comp Physiol* **298**: R1173-R1187
3. Chazaud B, Brigitte M, Yacoub-Youssef H, Arnold L, Gherardi R, Sonnet C, Lafuste P, Chretien F (2009) Dual and beneficial roles of macrophages during skeletal muscle regeneration. *Exerc Sport Sci Rev* **37**: 18–22
4. Murray PJ, Wynn TA (2011) Protective and pathogenic functions of macrophage subsets. *Nat Rev Immunol* **11**: 723–737
5. Tatsumi R, Anderson JE, Nevoret CJ, Halevy O, Allen RE (1998) HGF/SF is present in normal adult skeletal muscle and is capable of activating satellite cells. *Dev Biol* **194**: 114–128
6. Musaro A, Rosenthal N (1999) Maturation of the myogenic program is induced by postmitotic expression of insulin-like growth factor I. *Mol Cell Biol* **19**: 3115-3124
7. Lee SJ, McPherron AC (2001) Regulation of myostatin activity and muscle growth. *Proc Natl Acad Sci U S A* **98**: 9306-9311
8. Toschi A, Severi A, Coletti D, Catizone A, Musarò A, Molinaro M, Nervi C, Adamo S, Scicchitano BM (2011) Skeletal muscle regeneration in mice is stimulated by local overexpression of V1a-vasopressin receptor. *Mol Endocrinol* **25**: 1661-1673
10. von Maltzahn J, Chang NC, Bentzinger CF, Rudnicki MA (2012) Wnt signaling in myogenesis. *Trends Cell Biol* **22**: 602-609
11. Tedesco FS, Dellavalle A, Diaz-Manera J, Messina G, Cossu G (2010) Repairing skeletal muscle: regenerative potential of skeletal muscle stem cells. *J Clin Invest* **120**: 11–19
12. Braun T, Gautel M (2011) Transcriptional mechanisms regulating skeletal muscle differentiation, growth, and homeostasis. *Nat Rev Mol Cell Biol* **12**: 349–361
13. Gurriarán-Rodríguez U, Santos-Zas I, Al-Massadi O, Mosteiro CS, Beiroa D, Nogueiras R, Crujeiras AB, Seoane LM, Señarís J, García-Caballero T, Gallego R, Casanueva FF, Pazos Y, Camiña JP (2012) The obestatin/GPR39 system is up-regulated by muscle injury and functions as an autocrine regenerative system. *J Biol Chem* **287**: 38379-38389

14. Zatz M, Rapaport D, Vainzof M, Passos-Bueno MR, Bortolini ER, Pavanello Rde C, Peres CA (1991) Serum creatine-kinase (CK) and pyruvate-kinase (PK) activities in Duchenne (DMD) as compared with Becker (BMD) muscular dystrophy. *J Neurol Sci* **102**: 190-196
15. von Maltzahn J, Bentzinger CF, Rudnicki MA (2011) Wnt7a-Fzd7 signalling directly activates the Akt/mTOR anabolic growth pathway in skeletal muscle. *Nat Cell Biol* **14**: 186-191
16. Alvarez CJ, Lodeiro M, Theodoropoulou M, Camiña JP, Casanueva FF, Pazos Y (2009) Obestatin stimulates Akt signalling in gastric cancer cells through beta-arrestin-mediated epidermal growth factor receptor transactivation. *Endocr Relat Cancer* **16**: 599-611
17. Um SH, Frigerio F, Watanabe M, Picard F, Joaquin M, Sticker M et al (2004) Absence of S6K1 protects against age- and diet-induced obesity while enhancing insulin sensitivity. *Nature* **431**: 200–205
18. von Maltzahn J, Jones AE, Parks RJ, Rudnicki MA (2013) Pax7 is critical for the normal function of satellite cells in adult skeletal muscle. *Proc Natl Acad Sci U S A* **110**: 16474-16479
19. He WA, Berardi E, Cardillo VM, Acharyya S, Aulino P, Thomas-Ahner J, Wang J, Bloomston M, Muscarella P, Nau P, Shah N, Butchbach ME, Ladner K, Adamo S, Rudnicki MA, Keller C, Coletti D, Montanaro F, Guttridge DC (2013) NF- κ B-mediated Pax7 dysregulation in the muscle microenvironment promotes cancer cachexia. *J Clin Invest* 2013 pii: 68523. doi: 10.1172/JCI68523
20. Filigheddu N, Gnocchi VF, Coscia M, Cappelli M, Porporato PE, Taulli R, Traini S, Baldanzi G, Chianale F, Cutrupi S, Arnoletti E, Ghè C, Fubini A, Surico N, Sinigaglia F, Ponzetto C, Muccioli G, Crepaldi T, Graziani A (2007) Ghrelin and des-acyl ghrelin promote differentiation and fusion of C2C12 skeletal muscle cells. *Mol Biol Cell* **18**: 986–994
21. Porporato PE, Filigheddu N, Reano S, Ferrara M, Angelino E, Gnocchi VF, Prodám F, Ronchi G, Fagoonee S, Fornaro M, Chianale F, Baldanzi G, Surico N, Sinigaglia F, Perroteau I, Smith RG, Sun Y, Geuna S, Graziani A (2013) Acylated and unacylated ghrelin impair skeletal muscle atrophy in mice. *J Clin Invest* **123**: 611-622
22. Glass DJ (2005) Skeletal muscle hypertrophy and atrophy signaling pathways. *Int J Biochem Cell Biol* **37**: 1974-1984
23. Lee CH, Inoki K, Guan KL (2007) mTOR pathway as a target in tissue hypertrophy. *Annu Rev Pharmacol Toxicol* **47**: 443-67.
24. Bryan BA, Walshe TE, Mitchell DC, Havumaki JS, Saint-Geniez M, Maharaj A S, Maldonado AE, D'Amore PA (2008) Coordinated vascular endothelial growth factor expression and signaling during skeletal myogenic differentiation. *Mol Biol Cell* **19**: 994–1006

25. Messina S, Mazzeo A, Bitto A, Aguenouz M, Migliorato A, De Pasquale MG, Minutoli L, Altavilla D, Zentilin L, Giacca M, Squadrito F, Vita G (2007) VEGF overexpression via adeno-associated virus gene transfer promotes skeletal muscle regeneration and enhances muscle function in mdx mice. *FASEB J* **21**: 3737-3746
26. Deasy BM, Feduska JM, Payne TR, Li Y, Ambrosio F, Huard J (2009) Effect of VEGF on the regenerative capacity of muscle stem cells in dystrophic skeletal muscle. *Mol Ther* **17**: 1788-1798
27. Schuelke M, Wagner KR, Stolz LE, Hübner C, Riebel T, Kömen W, Braun T, Tobin JF, Lee SJ (2004) Myostatin mutation associated with gross muscle hypertrophy in a child. *N Engl J Med* **350**: 2682-2688
28. McCroskery S, Thomas M, Maxwell L, Sharma M, Kambadur R (2003) Myostatin negatively regulates satellite cell activation and self-renewal. *J Cell Biol* **162**:1135-1147
29. Wagner KR, Liu X, Chang X, Allen RE (2005) Muscle regeneration in the prolonged absence of myostatin. *Proc Natl Acad Sci U S A* **102**: 2519-2524
30. Li ZB, Kollias HD, Wagner KR (2008) Myostatin directly regulates skeletal muscle fibrosis. *J Biol Chem* **283**:19371-19378
31. Li ZB, Zhang J, Wagner KR (2012) Inhibition of myostatin reverses muscle fibrosis through apoptosis. *J Cell Sci* **125**:3957-3965
32. Halevy O, Novitsch BG, Spicer DB, Skapek SX, Rhee J, Hannon GJ, Beach D, Lassar AB (1995) Correlation of terminal cell cycle arrest of skeletal muscle with induction of p21 by MyoD. *Science* **267**: 1018-1021
33. Reynaud EG, Leibovitch MP, Tintignac LAJ, Pelpel K, Guillier M, Leibovitch SA (2000) Stabilization of MyoD by direct binding to p57(Kip2). *J Biol Chem* **275**:18767-18776.
34. Osborn DPS, Li K, Hinits Y, Hughes SM (2010) Cdkn1c drives muscle differentiation through a positive feedback loop with Myod. *Dev Biol* **350**:464-475.
35. Bigot A, Jacquemin V, Debacq-Chainiaux F, Butler-Browne GS, Toussaint O, Furling D, Mouly V (2008) Replicative aging down-regulates the myogenic regulatory factors in human myoblasts. *Biol Cell* **100**:189-199
36. Zalc A, Hayashi S, Auradé F, Bröhl D, Chang T, Mademtzoglou D, Mourikis P, Yao Z, Cao Y, Birchmeier C, Relaix F (2014) Antagonistic regulation of p57kip2 by Hes/Hey downstream of Notch signaling and muscle regulatory factors regulates skeletal muscle growth arrest. *Development* **141**:2780-2790
37. Leloup L, Daury L, Mazères G, Cottin P, Brustis JJ (2007) Involvement of the ERK/MAP kinase signalling pathway in milli-calpain activation and myogenic cell migration. *Int J Biochem Cell Biol* **39**: 1177–1189
38. Winter B, Arnold HH (2000) Activated raf kinase inhibits muscle cell differentiation through a MEF2-dependent mechanism. *J Cell Sci* **113**: 4211-4220

39. Gredinger E, Gerber AN, Tamir Y, Tapscott SJ, Bengal E (1998) Mitogen-activated protein kinase pathway is involved in the differentiation of muscle cells. *J Biol Chem* **273**: 10436-10444
40. Wu Z, Woodring PJ, Bhakta KS, Tamura K, Wen F, Feramisco JR, Karin M, Wang JY, Puri PL (2000) p38 and extracellular signal-regulated kinases regulate the myogenic program at multiple steps. *Mol Cell Biol* **20**: 3951-3964
41. Scicchitano BM, Spath L, Musarò A, Molinaro M, Rosenthal N, Nervi C, Adamo S (2005) Vasopressin-dependent myogenic cell differentiation is mediated by both Ca²⁺/calmodulin-dependent kinase and calcineurin pathways. *Mol Biol Cell* **16**: 3632-3641
42. Skelding KA, Rostas JA, Verrills NM (2011) Controlling the cell cycle: the role of calcium/calmodulin-stimulated protein kinases I and II. *Cell Cycle* **10**: 631-639
43. Wu M, Falasca M, Blough ER (2011) Akt/protein kinase B in skeletal muscle physiology and pathology. *J Cell Physiol* **226**: 29–36
44. Rotwein P, Wilson EM (2009) Distinct actions of Akt1 and Akt2 in skeletal muscle differentiation. *J Cell Physiol* **219**: 503-511
45. Sandri M, Sandri C, Gilbert A, Skurk C, Calabria E, Picard A, Walsh K, Schiaffino S, Lecker SH, Goldberg AL (2004) Foxo transcription factors induce the atrophy-related ubiquitin ligase atrogin-1 and cause skeletal muscle atrophy. *Cell* **117**: 399-412
46. Stitt TN, Drujan D, Clarke BA, Panaro F, Timofeyeva Y, Kline WO, Gonzalez M, Yancopoulos GD, Glass DJ (2004) The IGF-1/PI3K/Akt pathway prevents expression of muscle atrophy-induced ubiquitin ligases by inhibiting FOXO transcription factors. *Mol Cell* **14**: 395–403
47. Lluís F, Perdiguero E, Nebreda AR, Muñoz-Cánoves P (2006) Regulation of skeletal muscle gene expression by p38 MAP kinases. *Trends Cell Biol* **16**: 36-44.
48. Perdiguero E, Ruiz-Bonilla V, Gresh L, Hui L, Ballestar E, Sousa-Victor P, Baeza-Raja B, Jardí M, Bosch-Comas A, Esteller M, Caelles C, Serrano AL, Wagner EF, Muñoz-Cánoves P (2007) Genetic analysis of p38 MAP kinases in myogenesis: fundamental role of p38alpha in abrogating myoblast proliferation. *EMBO J* **26**: 1245-1256
49. Perdiguero E, Ruiz-Bonilla V, Serrano AL, Muñoz-Cánoves P (2007) Genetic deficiency of p38alpha reveals its critical role in myoblast cell cycle exit: the p38alpha-JNK connection. *Cell Cycle* **6**: 1298-12303

50. Serra C, Palacios D, Mozzetta C, Forcales SV, Morantte I, Ripani M, Jones D R, Du K, Jhala US, Simone C, Puri PL (2007) Functional interdependence at the chromatin level between the MKK6/p38 and IGF1/PI3K/AKT pathways during muscle differentiation. *Mol Cell* **28**: 200–213
51. Alén BO, Nieto L, Gurriarán-Rodríguez U, Mosteiro CS, Álvarez-Pérez JC, Otero-Alén M, Camiña JP, Gallego R, García-Caballero T, Martín-Pastor M, Casanueva FF, Jiménez-Barbero J, Pazos Y (2012) The NMR structure of human obestatin in membrane-like environments: insights into the structure-bioactivity relationship of obestatin. *PLoS One* **7**:e45434
52. Zoncu R, Efeyan A, Sabatini DM (2011) mTOR: from growth signal integration to cancer, diabetes and ageing. *Nat Rev Mol Cell Biol* **12**: 21-35
53. Santos-Zas I, Lodeiro M, Gurriarán-Rodríguez U, Bouzo-Lorenzo M, Mosteiro CS, Casanueva FF, Casabiell X, Pazos Y, Camiña JP (2013) β -Arrestin signal complex plays a critical role in adipose differentiation. *Int J Biochem Cell Biol* **45**:1281-1292
54. Chargé SB, Brack AS, Hughes SM (2002) Aging-related satellite cell differentiation defect occurs prematurely after Ski-induced muscle hypertrophy. *Am J Physiol Cell Physiol* **283**: C1228-1241
55. Le Grand F, Jones AE, Seale V, Scimè A, Rudnicki MA (2009) Wnt7a activates the planar cell polarity pathway to drive the symmetric expansion of satellite stem cells. *Cell Stem Cell* **4**: 535-547

FIGURE LEGENDS

Figure 1 Ectopic expression of preproghrelin enhances muscle regeneration. (a) *Upper panel*, immunoblot analysis revealed comparable levels of pERK1/2(T202/Y204) and pAkt(S473) under HA-obestatin stimulation (5 nM, 10 min) to obestatin-treated C2C12 myoblast cells (5 nM, 10 min). *Lower panel*, immunoprecipitation analyses using GFP coupled beads demonstrated that GPR39-GFP binds obestatin-HA in C2C12 myoblast cells while it does not bind GFP alone. (b) Representative histology sections of transfected muscle 96- and 168-h after electroporation with CMV plasmid in TA. (c) *Left panel*, fluorescence microscopy of GFP (pcDNA 3.1-SNAP-GFP, transfection marker) and immunofluorescence analysis of cryosections stained with specific antibodies reactive to laminin and preproghrelin 168-h after electroporation with the CMV-preproghrelin plasmid in TA. *Right panel*, representative immunoblots of the mean values from each group of the expression of Pax-7, MyoD, myogenin, and eMHC at 96- and 168-h after ectopic expression of preproghrelin. *Bottom panel*, immunoblot analysis of the expression of Pax-7, MyoD, myogenin, and MHC at 96- and 168-h after ectopic expression of preproghrelin. Protein levels were expressed as fold of control obtained from electroporation of CMV plasmid group (n=5/group). Data were expressed as mean±SEM obtained from intensity scans. * $P < 0.05$ versus control values.

Figure 2 Ectopic expression of GPR39 or preproghrelin/GPR39 enhances muscle regeneration. (a) *Left panel*, fluorescence microscopy of GFP (pcDNA 3.1-SNAP-GFP, transfection marker) and immunofluorescence analysis of cryosections stained with antibodies reactive to laminin and GPR39 168-h after electroporation with the CMV-GPR39 plasmid. *Middle panel*, representative immunoblots of the mean values from each group of the expression of Pax-7, MyoD, myogenin, and eMHC at 96- and 168-h after ectopic expression of

GPR39. *Right panel*, immunoblot analysis of the expression of Pax-7, MyoD, myogenin, and MHC at 96- and 168-h after ectopic expression of GPR39. **(b)** *Left panel*, fluorescence microscopy of GFP (pcDNA 3.1-SNAP-GFP, transfection marker) and immunofluorescence analysis of the cryosections stained with antibodies reactive to laminin, preproghrelin or GPR39 168-h after electroporation with both CMV-GPR39 and CMV-preproghrelin plasmids. *Right panel*, representative immunoblots of the mean values from each group of the expression of Pax-7, MyoD, myogenin, and MHC at 96- and 168-h after ectopic expression of GPR39. *Bottom panel*, immunoblot analysis of the expression of Pax-7, MyoD, myogenin, and eMHC at 96- and 168-h after ectopic expression of GPR39 and preproghrelin. For **a** and **b**, protein levels were expressed as fold of control obtained from electroporation of CMV plasmid group (n=5/group). Data were expressed as mean \pm SEM obtained from intensity scans. * P <0.05 versus control values.

Figure 3 Intramuscular obestatin administration enhances muscle regeneration. **(a)** *Upper panel*, immunofluorescence analysis of the obestatin dispersion in the distal zone from the injection site [obestatin-HA: 300 nmol/kg body weight; 30 min after administration]. *Lower panel*, immunofluorescence analysis of pAkt(S473) of distal cross-sections of obestatin-HA-injected TA, contralateral TA and control TA muscles. Cryosections were stained with antibodies reactive to HA-tag, laminin, pAkt(S473) and counterstained with DAPI 30-min after injection of HA-obestatin. **(b)** Representative images of hematoxylin/eosin-stained sections of resting (control) and freeze-injured TA muscles after intramuscular injection of obestatin [300 nmol/kg body weight/24-h during 5 days; n=5 per time point] or vehicle (PBS) at 48-, 96-, 168- and 240-h following injury. **(c)** Effect of intramuscular injection of obestatin [300 nmol/kg body weight/24 h] on regenerating myofiber (centrally located nuclei) cross-section area at 96 and 168 hours following injury. **(d)** Cross-sectional area measurements of freeze-injured TA

muscles after intramuscular injection of obestatin [300 nmol/kg body weight/24-h during 5 days; n=5 per group] at 240 hours following injury. (e) Representative immunoblots of the mean values from each group of the expression of Pax-7, MyoD, myogenin, and eMHC in freeze-injured TA muscles after intramuscular injection of obestatin or vehicle (PBS) at 48-, 96-, 168- and 240-h following injury. (e-i) Immunoblot analysis of the expression of Pax-7 (f), MyoD (g), myogenin (h), and eMHC (i) in resting (control) and freeze-injured TA muscles after intramuscular injection of obestatin [300 nmol/kg body weight/24-h during 5 days; n=5 per time point] or vehicle (PBS) at 48-, 96-, 168- and 240-h following injury. Protein levels were expressed as fold of control (n=5/group). Data were expressed as mean±SEM obtained from intensity scans. *,# $P < 0.05$ versus control values. (j) Representative immunofluorescence images of eMHC in freeze-injured TA muscles after intramuscular injection of obestatin [300 nmol/kg body weight/24-h during 5 days; n=5 per time point] or vehicle (PBS) at 96-h following injury. (k) Serum creatine kinase (CK) levels at 96-h post-injury (n=15 per group). Results are * $P < 0.05$ versus control values.

Figure 4 Obestatin activates SCs and increases the number of nuclei per muscle fiber.

(a) Average number of myonuclei per 100 TA muscle fibers after intramuscular injection of obestatin [300 nmol/kg body weight/24h during 5 days; n=5 per group] or control (PBS) at 240 hours following injury (n=5 per group). (b) Sample section for Pax7 and laminin in freeze-injured TA muscle after intramuscular injection of obestatin [300 nmol/kg body weight/24-h during 5 days; n=5 per group] or control (PBS) at 96-h following injury (left panel). Colocalization of Pax7 and DAPI staining from boxed region is shown in the middle panel. The analysis of the relative satellite cell density (ratio of satellite cell number to the cross-section area and normalized to the ratio in control muscles) is shown at 96-h following injury. Results were calculated from the average values of 3 muscle sections per mouse, and 5 mice were

analyzed (right panel). **(c)** *Left panel*, immunofluorescence analysis of Pax7 positive satellite cells (Pax7⁺) in myofibers isolated from the neighboring area of the injured zone of the TA muscle after intramuscular injection of obestatin [300 nmol/kg body weight/24h during 5 days; n=5 per group] or control (PBS) at 96-h following injury. *Right panel*, Pax7⁺ cells were enumerated and normalized against myofiber length (μm). Results were calculated from average values of 12 isolated myofibers per mouse, and 5 mice were analyzed per group (n=60 per group). Data were expressed as mean \pm SEM. * $P < 0.05$ versus control values.

Figure 5 Effect of obestatin administration on muscle force. Obestatin or PBS (vehicle) was administered via intramuscular injection in freeze-injured TA muscle (300 nmol/kg body weight/24h during 5 days). Uninjured TA muscles were taken as control to establish that the damage area was large enough to decrease force (n=6 per group). Muscle force measurements were assessed after an interval of 5 days after the last dose. **(a)** Effect of intramuscular injection of obestatin on twitch force at 240 h following injury. **(b)** Effect of intramuscular injection of obestatin on tetanic force at 240 h following injury. **(c)** Force-frequency curve of TA muscles in control and obestatin- or PBS-treated groups. Data in **(a-c)** were expressed as mean \pm SEM. * $P < 0.05$ versus control values.

Figure 6 Obestatin regulates the regenerative microenvironment responsible for stimulating and coordinating skeletal muscle repair. Effect of intramuscular injection obestatin [300 nmol/kg body weight/24h during 5 days; n=5 per group] or control (PBS) in freeze-injured TA muscle on Ki67 **(a)**, Cyclin D1 **(b)**, VEGF **(c)**, VEGF-R2 **(d)**, average number of isolectin positive vessels (isolectin+) **(e)**, Col1a2 **(f)**, and myostatin **(g)** at 96 or 240 hours following injury. Analysis of the expression of Ki67, Cyclin D1, VEGF, VEGF-R2, Col1a2 and myostatin were performed by immunoblot and protein levels were expressed as fold of control

(n=5 per group). Immunoblots are representative of mean values from each group. Data were expressed as mean \pm SEM obtained from intensity scans. Isolectin positive vessels were analyzed by immunofluorescence of cryosections stained with isolectin, laminin and counterstained with DAPI. Representative images of the mean values from each group are shown in the upper panel from (e). Representative images of the histological analysis from sections stained with Heidenhain's AZAN trichrome staining are shown in the bottom panel from (f). * $P < 0.05$ versus control values.

Figure 7 Obestatin effect on cell proliferation. (a) Dose-response effect of obestatin (0.01-100 nM) on C2C12 myoblast cell proliferation (48 h, n=5). Co: cells initially seeded. Control: cells maintained 48 h in GM. (b) Immunoblot analysis of Ki67, p57, p21, myogenin, and MHC expression in the course of C2C12 myogenesis under DM or DM+obestatin (5 nM). Protein level was expressed as fold of control cells in GM (n=3). Immunoblots are representative of the mean value. Data were expressed as mean \pm SEM obtained from intensity scans. * $P < 0.05$ versus control values.

Figure 8 The hypertrophic response to obestatin is not associated with the addition of new myonuclei via proliferation and further fusion. (a) *Left panel*, immunofluorescence detection of MHC and DAPI in C2C12 myotube cells under DM (control) or DM+obestatin (5 nM) at the 7-day point after stimulation. *Right panel*, the myotube area (μm^2) and the number of nuclei within individual myotubes (at least two nuclei) were evaluated. (b) *Left panel*, immunofluorescence detection of MHC and DAPI in C2C12 myotube cells under DM (control) or DM+obestatin (5 nM; 3 days of differentiation) at the 7-day point after stimulation. *Right panel*, the myotube area (μm^2) and the number of nuclei within individual myotubes were evaluated. (c) *Left panel*, immunofluorescence detection of MHC and DAPI in C2C12 myotube

cells at 7-day point after stimulation under DM (control) or DM+obestatin (5 nM)+AraC (50 μ M) applied at day three of differentiation. *Right panel*, the myotube area (μm^2) and the number of nuclei within individual myotubes (at least two nuclei) were evaluated. **(d)** Immunoblot analysis of myogenin, and MHC expression in C2C12 myotubes at the 7-day point after stimulation under AraC treatment as indicated in **(c)**. Immunoblots are representative of mean values from each group. Data were expressed as mean \pm SEM obtained from intensity scans. * $P < 0.05$ versus control values.

Figure 9 Obestatin-activated intercellular networks involved during myogenic program in C2C12 cells. **(a)** Immunoblot analysis of pAkt(S473), pERK1/2(T202/Y204), pp38(T180/Y182), pS6K1(S6371), pFoxO1(T24)/FoxO3a(T32), pCAMKII(T286), and, pc-Jun(S63) in the course of C2C12 myogenesis under DM or DM+obestatin (5 nM). **(b)** Immunoblot analysis of pIGFR(Y1316) and pIRS1(S636/639) in the course of C2C12 myogenesis under DM or DM+obestatin (5 nM). For **(a)** and **(b)**, protein level was expressed as fold of control cells in GM (n=5). Immunoblots are representative of the mean value. Data were expressed as mean \pm SEM obtained from intensity scans. * $P < 0.05$ versus control values.

Figure 10 Obestatin-activated intercellular networks involved during myogenic program in TA muscle 96-h following injury. **(a)** Immunoblot analysis of pAkt(S473), pERK1/2(T202/Y204), pp38(T180/Y182), pS6K1(S6371), pFoxO1(T24)/FoxO3a(T32), pCAMKII(T286), and, pc-Jun(S63) in freeze-injured TA muscles after intramuscular injection of obestatin [300 nmol/kg body weight/24-h during 5 days; n=5] or vehicle (PBS) at 96 hours following injury. **(b)** Immunoblot analysis of pIGFR(Y1316) and pIRS1(S636/639) in freeze-injured TA muscles after intramuscular injection of obestatin [300 nmol/kg body weight/24h

during 5 days; n=5] or vehicle (PBS) at 96 hours following injury. For **(a)** and **(b)**, protein level was expressed as fold of control TA muscle (n=5 per group). Immunoblots are representative of the mean value. Data were expressed as mean±SEM obtained from intensity scans. * $P < 0.05$ versus control values.

Accepted manuscript

Figure 1

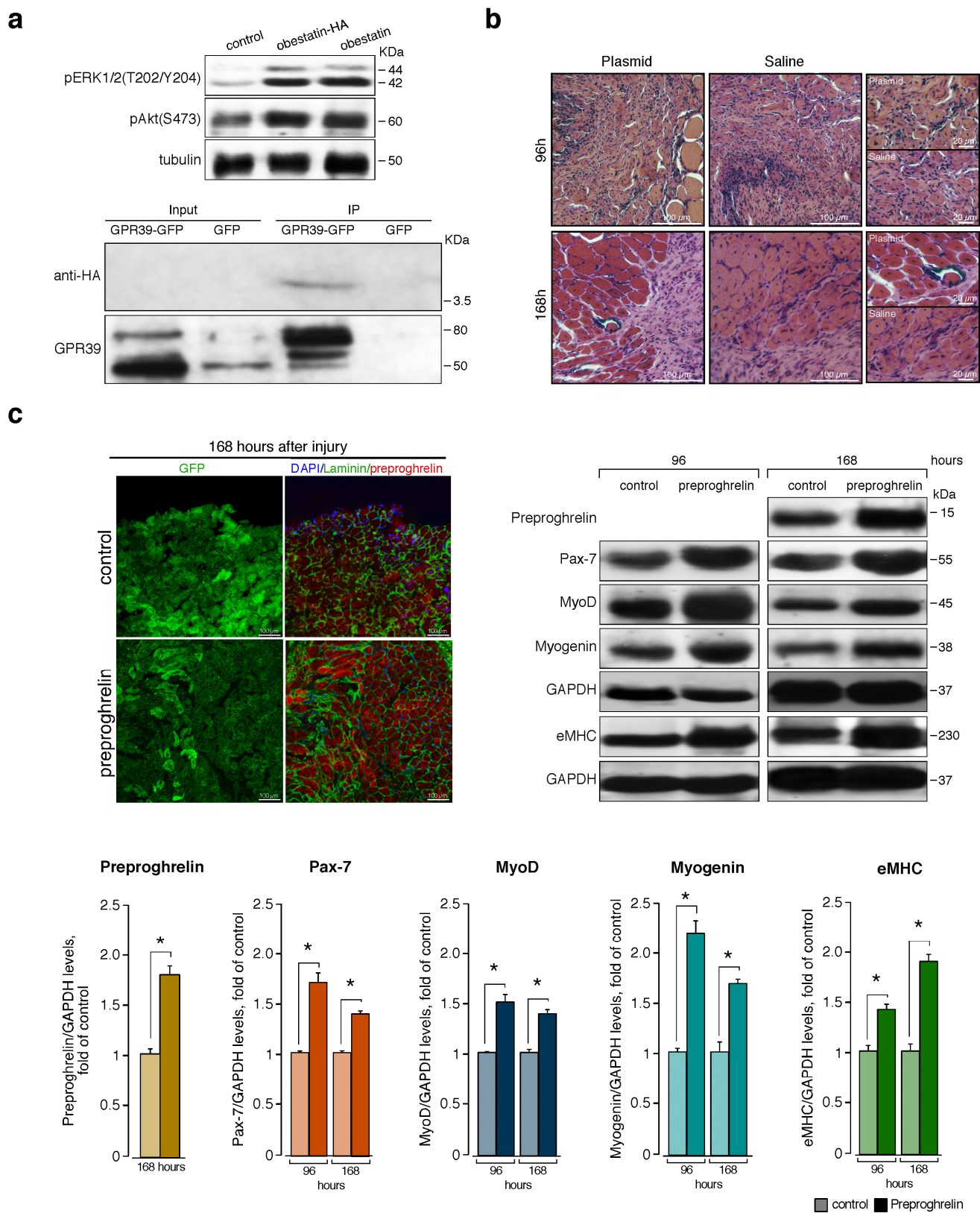


Figure 2

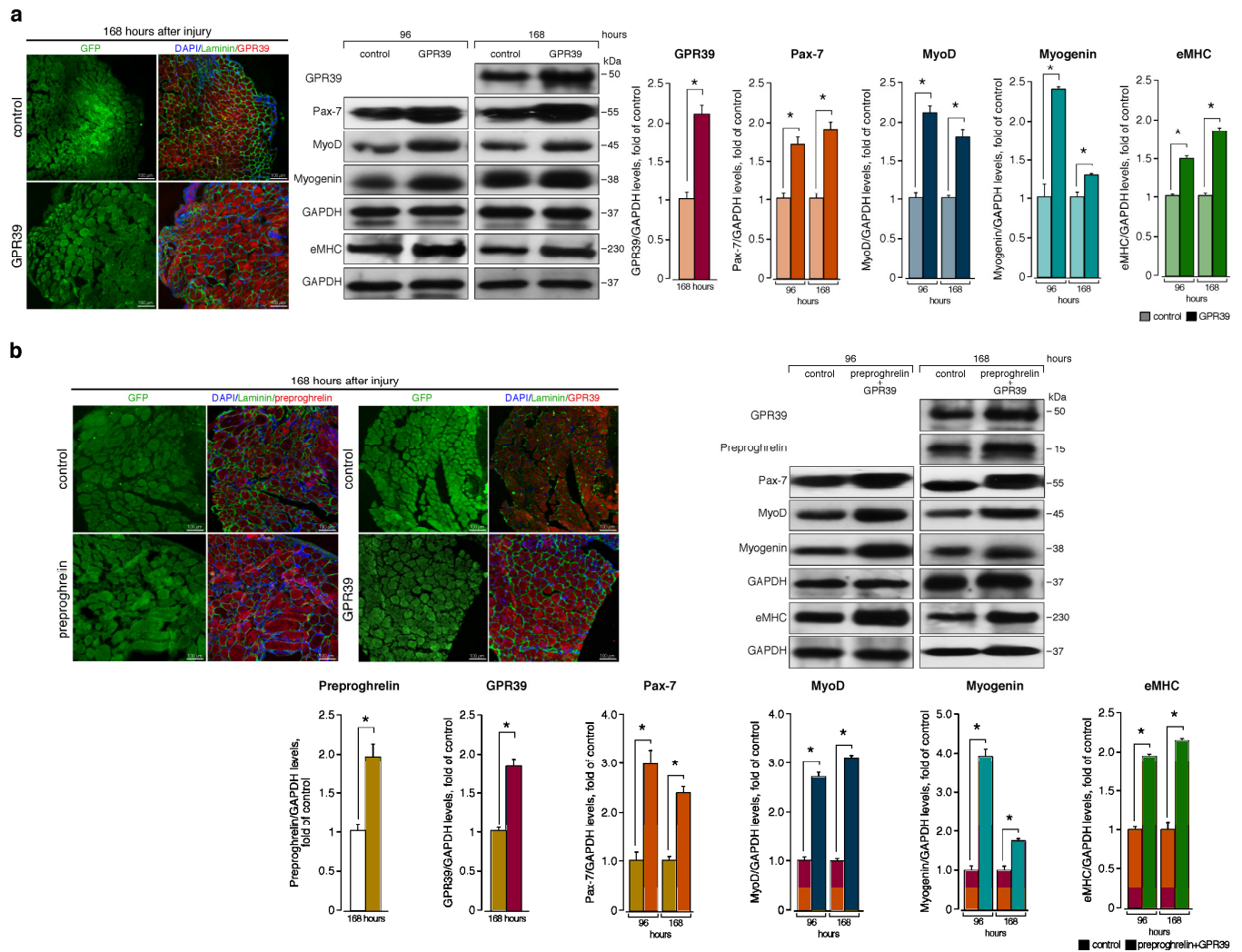


Figure 3

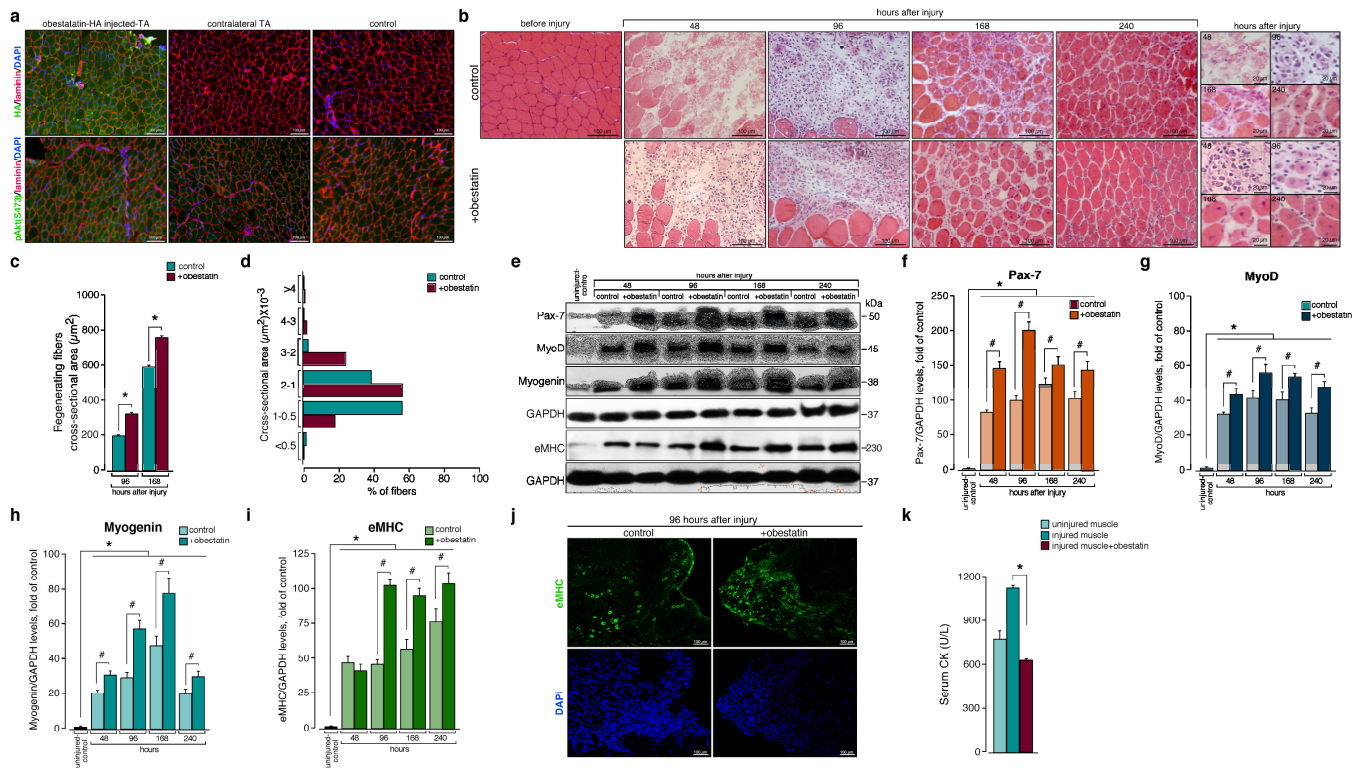


Figure 4

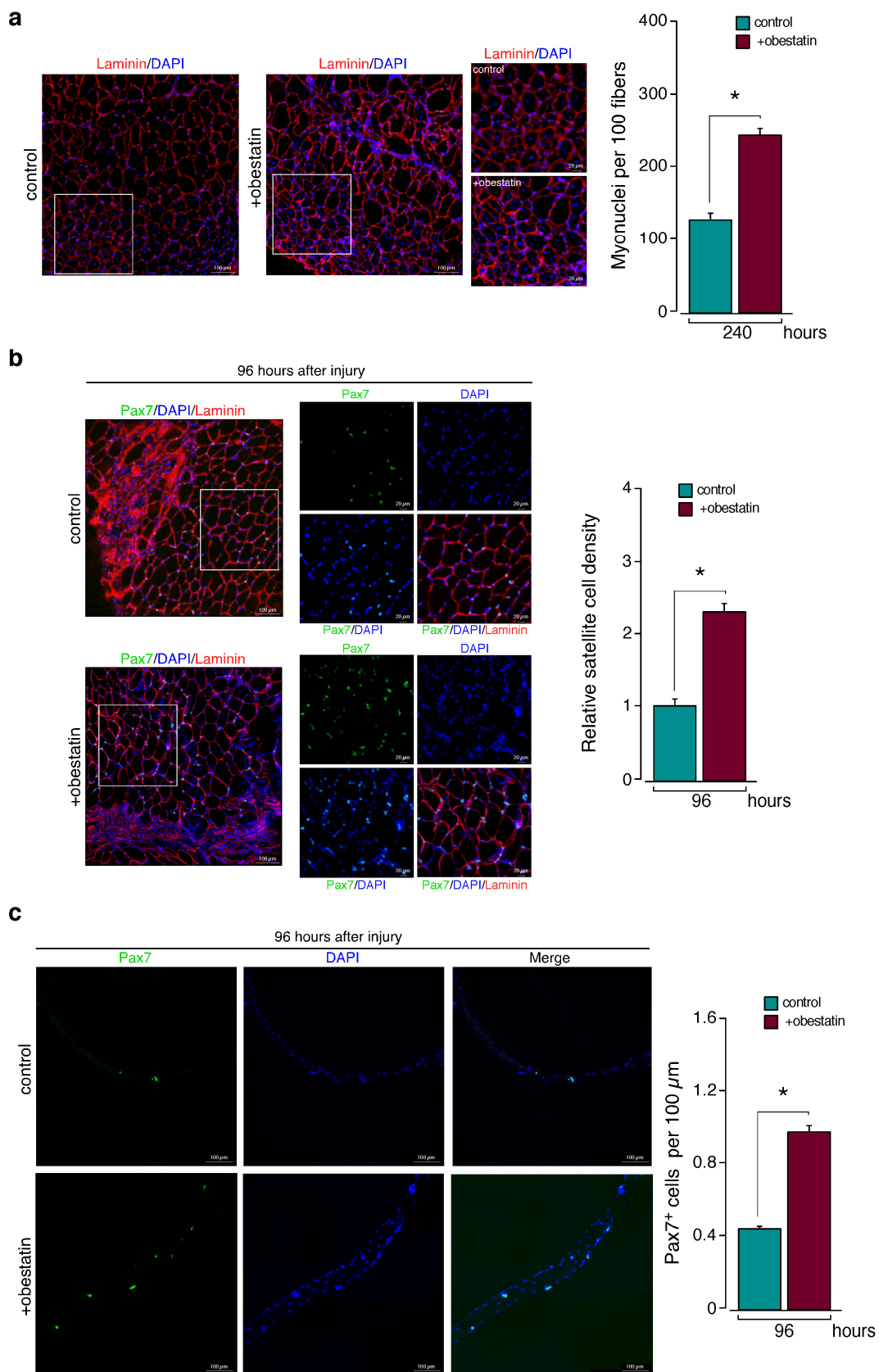


Figure 5

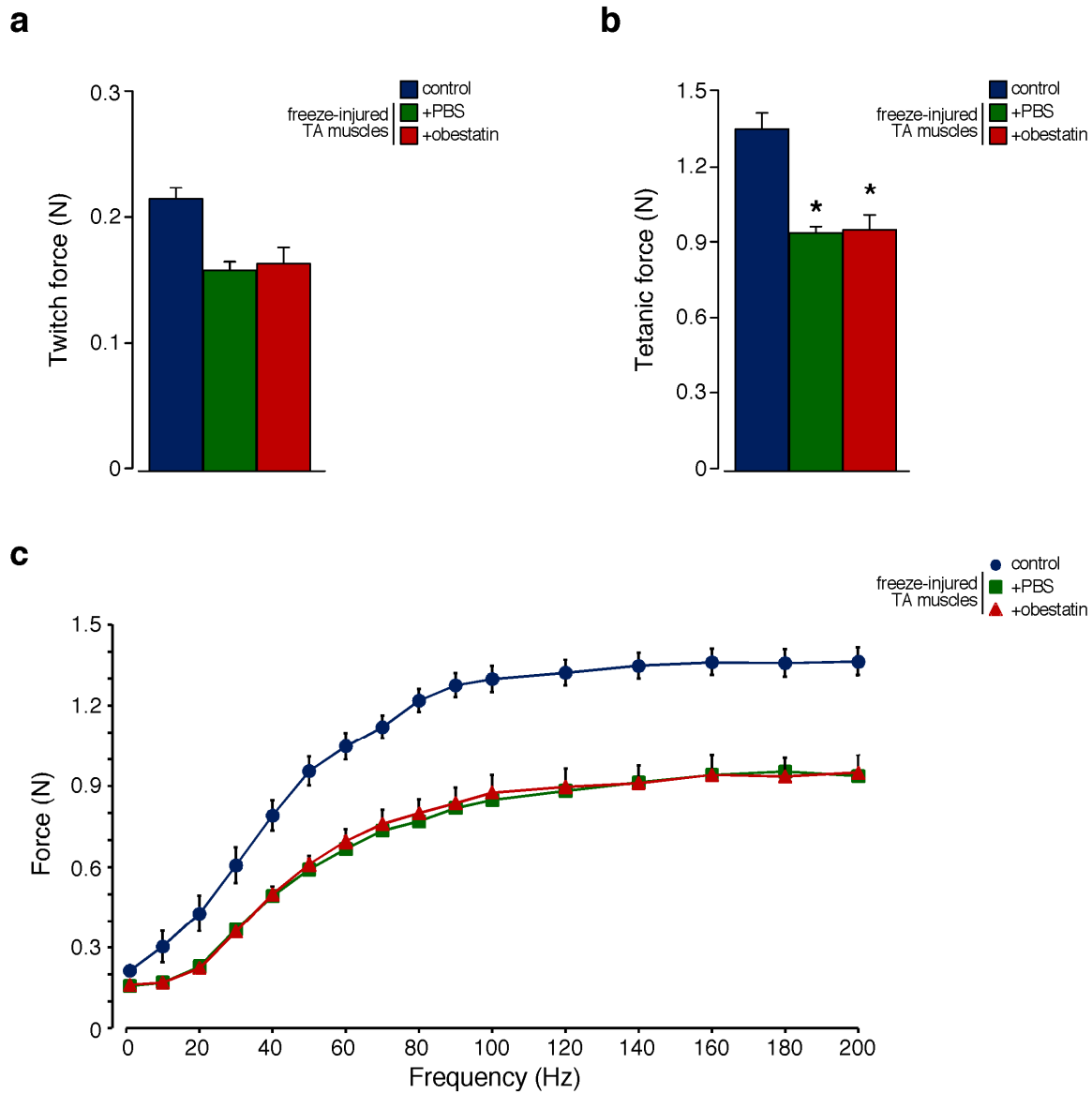


Figure 6

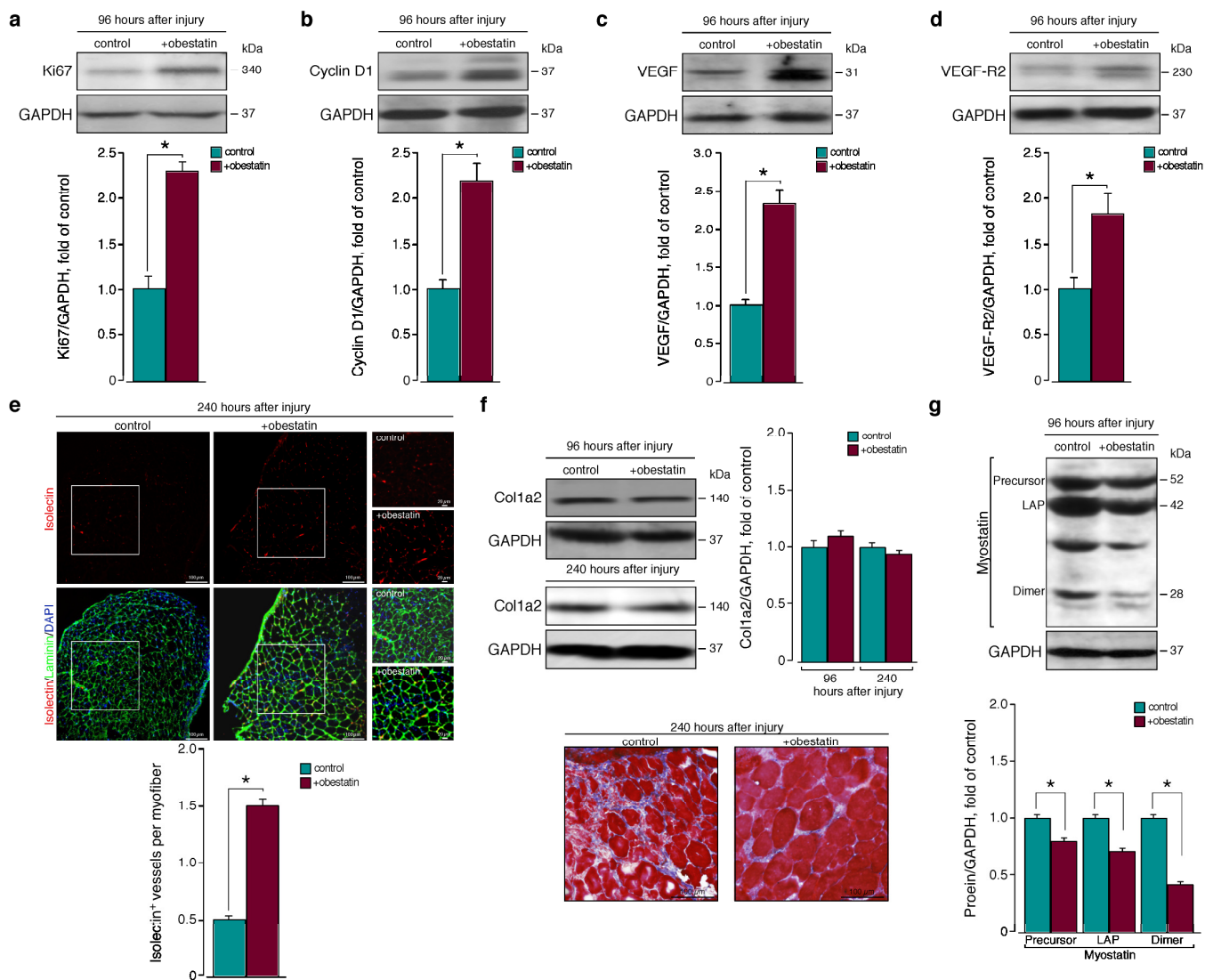


Figure 7

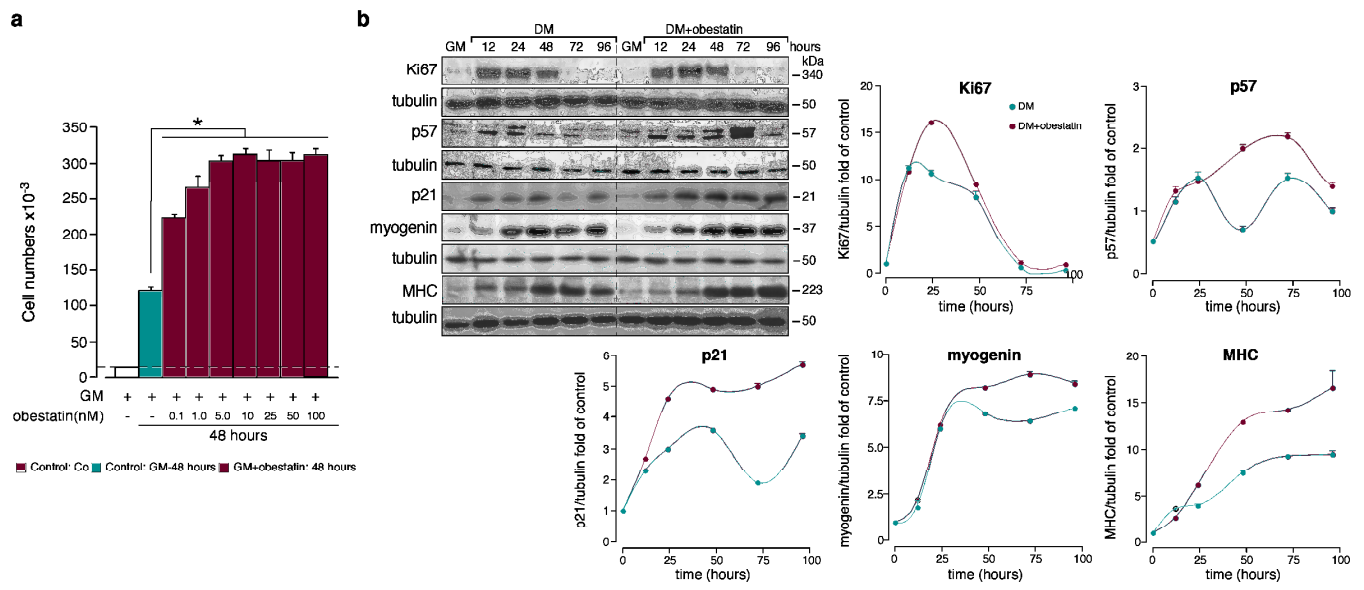


Figure 8

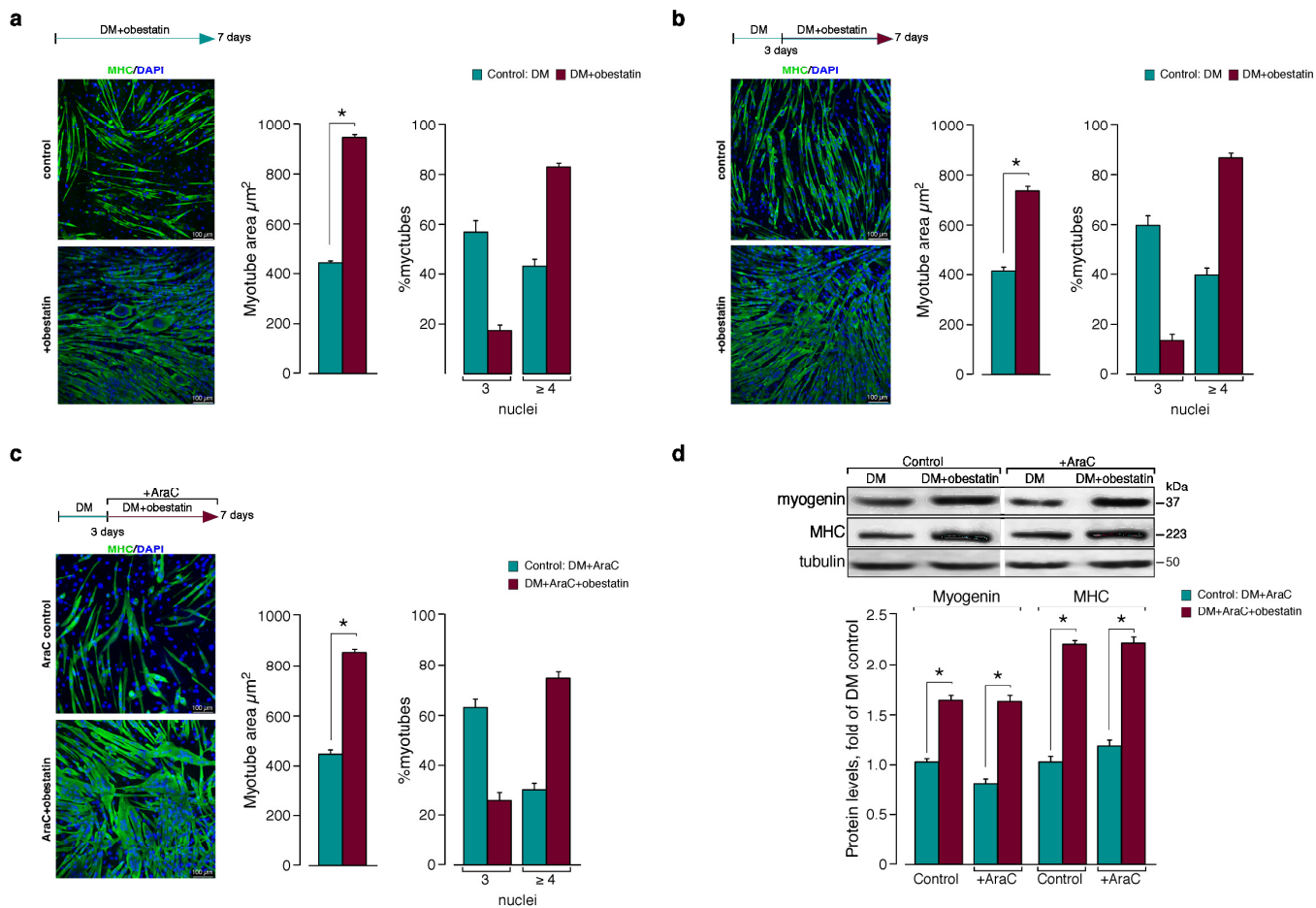


Figure 9

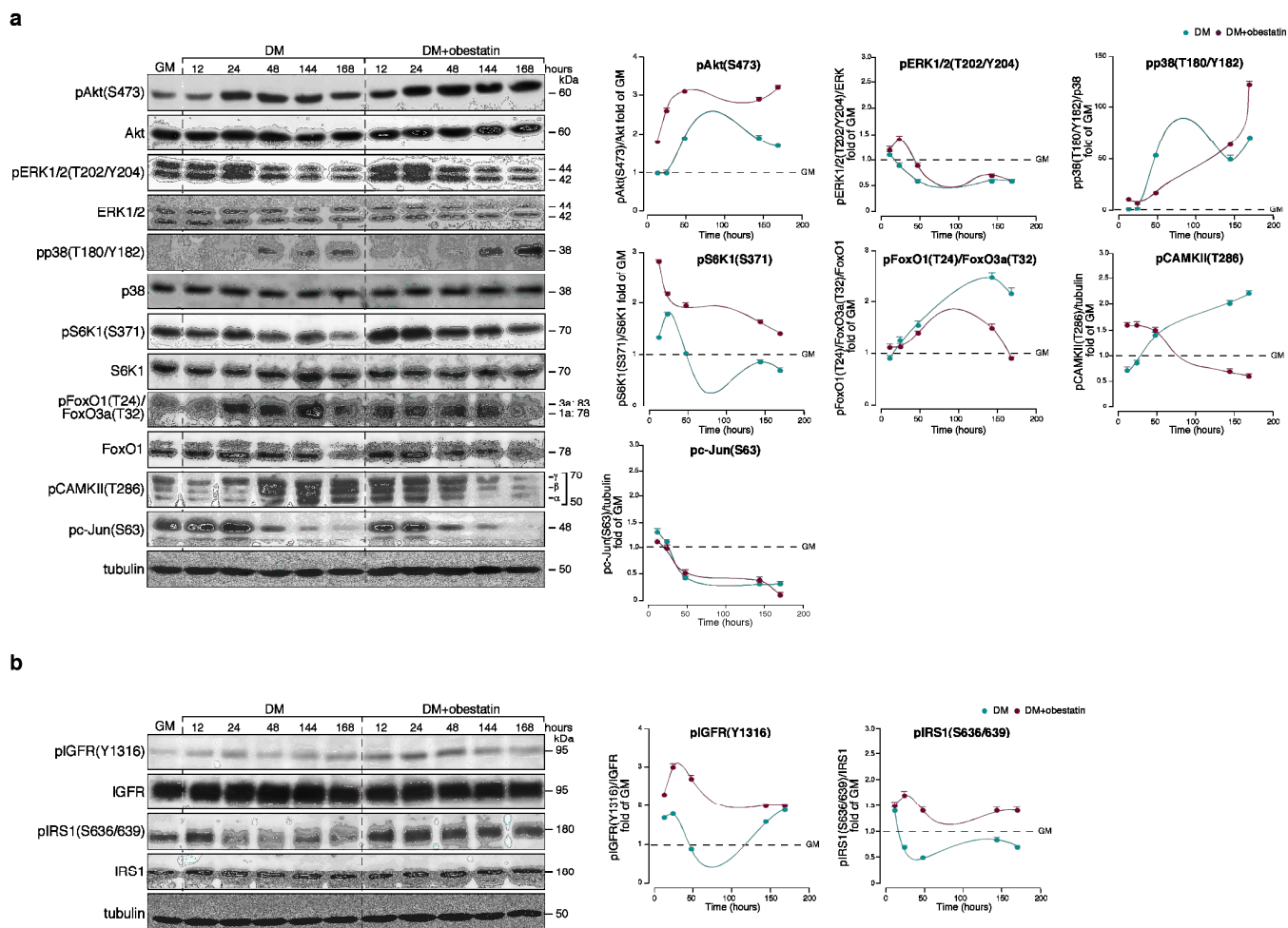


Figure 10

